AN ABSTRACT OF THE THESIS OF

Dakota Dailey for the degree of Master of Science in Kinesiology presented on June 11, 2020.

Title: Associations Between the PlayerLoad™ Metric and Common IMU-based Physical Activity-Related Measures of Human Movement

Abstract approved: _____

John M Schuna Jr.

Over the last 60 years, supplemental strength and conditioning for improving sport performance has gone from being nearly non-existent to a cornerstone feature of elite collegiate, amateur, and professional athletics. Concurrent with this profession-related evolution, technologies for monitoring and tracking physical performance have become more prevalent and useful. As an example, the Optimeye S5 from Catapult Sports is currently the most widely used sport performance-related inertial measurement unit (IMU) available for monitoring sport-related movement and is used by more than 2,500 athletic teams globally. The primary metric of interest quantified by this device is known as PlayerLoad™. PlayerLoad™ represents a cumulative summarization of changes in acceleration across three axes of measurement. Although somewhat similar in its formulation to commonly used physical activity-related acceleration metrics, such as band pass filtered Euclidean norm (BFEN) and Euclidean norm minus one (ENMO), no published reports have evaluated the associations between PlayerLoad™ and any of the aforementioned measures. We obtained two publicly available data sets (REAListic DISPlacement [REALDISP] and MHEALTH) containing high resolution IMU data. The REALDISP data set contained data from 17 participants (10 males, ages 22 to 37 years-old) completing 33 unique activities while wearing 9 IMUs across the body (upper-back; right and

left side: upper-arm, lower-arm, thigh, and calf). The MHEALTH data set contained data from 10 participants completing 11 unique activities while wearing 3 IMUs (right wrist, left pectoral, left ankle). Raw acceleration data collected from the IMUs was used to compute per second summaries of PlayerLoad™, BFEN, and ENMO. Association analyses revealed that PlayerLoad™ was highly correlated with BFEN and ENMO at all evaluated IMU locations ($r$ = 0.742 to 0.983); however, the strength of these associations did significantly vary across many locations. Notably, lower-body IMU measurement locations ($r$ = 0.951 to 0.983) generally produced higher correlations for PlayerLoad™ with BFEN and ENMO than did upper-body locations ($r$ = 0.742 to 0.960). Models were also developed for predicting epoch- and summary-level PlayerLoad™ from BFEN and ENMO. Unbiased pseudo $R^2$ values exceeded 0.879 in all instances indicating high predictive ability for all models. More research is needed to better understand PlayerLoad™ and its potential value for quantifying time-based dosages of human movement.

# Associations Between the PlayerLoad™ Metric and Common IMU-based Physical Activity-Related Measures of Human Movement

by
Dakota Dailey

A THESIS

Submitted to

Oregon State University

in partial fulfillment of
the requirements for the
degree of

Master of Science

Presented June 11, 2020
Commencement June 2020

Master of Science thesis of Dakota Dailey presented on June 11, 2020.

APPROVED:

Major Professor, representing Kinesiology

Head of the School of Biological and Population Health Sciences

Dean of the Graduate School

I understand that my thesis will become part of the permanent collection of Oregon State University libraries. My signature below authorizes release of my thesis to any reader upon request.

Dakota Dailey, Author

ACKNOWLEDGEMENTS

A special thank you to Bryan Klobuchar for his patience in teaching me the finer details of Catapult and their system. Also, for his willingness to share resources that have improved my understanding of how to monitor athletes as well as the devices themselves.

I am also grateful to coach Michael McDonald for allowing me a flexible enough schedule to work with the team and continue research simultaneously.

Finally, to my parents, David and Annie Dailey, none of this would have been possible without your continued support of my aspirations and goals, thank you both so much.

TABLE OF CONTENTS

LIST OF FIGURES

LIST OF TABLES

LIST OF APPENDICES

# LIST OF ABBREVIATIONS

ECG.....Electrocardiography

EKG .....Electrocardiography

BFEN .....Band pass filtered Euclidean norm

ENMO.....Euclidean norm minus one

GLONASS .....Global Navigation Satellite System, Russia

GNSS .....Global Navigation Satellite System

GPS .....Global Positioning System

IMU.....Inertial measurement unit

LFE .....Low-frequency extension

MAE.....Mean absolute error

MEMS.....Micro-electromechanical systems

MHEALTH.....Mobile health

MIMU .....Magnetic and inertial measurement unit

NF .....Normal filter

PPG .....Photoplethysmography

REALDISP .....REAListic sensor DISPlacement

RMSE.....Root mean squared error

SWA.....SenseWear armband

VM .....Vector magnitude

VMLFE .....Vector magnitude low-frequency extension activity counts

VMNF .....Vector magnitude normal filter activity counts

# Chapter 1. Introduction

## Background and Significance

Since the mid-20th century, professional and collegiate coaches have augmented traditional sport-based practice with supplemental aerobic, anaerobic, or resistance training exercise to enhance athletic performance. This supplemental exercise is intended to complement traditional sport-specific practices geared toward developing appropriate skill sets and techniques. One of the first examples of such supplemental physical training in professional sports was the 1963 San Diego Chargers football team which became the first professional program to implement a resistance training regimen and employ a strength and conditioning coach (George, 1993). Several years later, University of Nebraska football became the first collegiate program to employ a full-time strength and conditioning coach while implementing a comprehensive resistance training regimen (Shurley & Todd, 2012). Since the 1960s, the strength and conditioning profession has grown immensely such that most of today's professional and collegiate athletes partake in regular supplemental exercise supervised by strength and conditioning professionals.

Presently there are a variety of tools available to the strength and conditioning professional for monitoring the intensity and volume of supplemental exercise. The primary intent of such measurement tools is to inform the strength and conditioning professional's modulation of the exercise prescription while attempting to maximize desired training adaptations. Examples of these tools include heart rate monitors, cycling power meters, and rotary encoder-based power meters, among many others. The first commercially available wireless heart rate monitor was introduced by Polar® in 1982 (Polar, 2017). Since then, heart rate monitors have been used extensively in aerobic-based athletics for tracking heart rate as a

primary indicator of exercise intensity. Following the introduction of wireless heart rate monitors, the first spider-based cycling power meters for use with traditional bicycles were invented and developed in the mid-to-late 1980s (SRM GMBH, 2015). These power meters have now become commonplace and are used extensively among both professional and recreational cyclists for tracking cycling workload and peak power outputs (Passfield, Hopker, Jobson, Friel, & Zabala, 2017). Of more use to strength and power athletes, seminal research in the 1990s introduced rotary encoders to track implement displacement, velocity, and associated power during high-velocity resistance exercise (Humphries, Newton, & Wilson, 1995; Murphy, Wilson, Pryor, & Newton, 1995). Findings from this research informed the now widespread use of rotary encoder systems (e.g., TENDO units) for identifying optimal resistance training loads to maximize power output.

Over the last 10 to 15 years, wearable technologies (i.e., accelerometers, gyroscopes, magnetometers, Global Positioning System [GPS] devices, etc.) for measuring various aspects of athletic performance have become increasingly prevalent (Camomilla, Bergamini, Fantozzi, & Vannozzi, 2018). This trend has been fueled by the development and evolution of micro-electromechanical systems (MEMS) technology over the last 20 to 30 years. Current MEMS technology allows for the manufacture of highly miniaturized and power efficient sensors (e.g., gyroscopes, magnetometers, accelerometers) at relatively low costs (Camomilla et al., 2018). When attached to the body, these individual sensors can be used to obtain information about the body's movement and orientation. However, when orientation is estimated by only one type of sensor the measurement's accuracy may be inadequate for some applications (Sabatini, 2011). As such, to improve the accuracy of orientation estimations, usage of an inertial measurement unit (IMU) with 2-dimensions (i.e., accelerometer and gyroscope) or 3-dimentions (i.e.,

accelerometer, gyroscope, and magnetometer – sometimes referred to as a magnetic and inertial measurement unit [MIMU]) is preferred (Luinge & Veltink, 2005; Sabatini, 2005). IMU and MIMU units can also be integrated with other sensors such as GPS, heart rate monitors, and temperature sensors to assess outcomes such as energy expenditure or activity intensity. Of note, it is commonplace to refer to IMU and MIMU devices collectively as IMU devices.

Currently, the most commonly used IMU systems for assessing human movement in sport and athletic applications are manufactured and sold by Catapult Sports (Catapult Group International Ltd, Melbourne, Australia). The Optimeye S5 is the most commonly used Catapult IMU system and its capabilities have been previously evaluated among athletes in rugby (Hulin, Gabbett, Johnston, & Jenkins, 2017; Roe et al., 2017), ice hockey (Van Iterson, Fitzgerald, Dietz, Snyder, & Peterson, 2017), handball (Luteberget, Holme, & Spencer, 2018), and American football (Govus, Coutts, Duffield, Murray, & Fullagar, 2018; Li, Salata, Rambhia, Sheehan, & Voos, 2020; Murray, Buttfield, Simpkin, Sproule, & Tuner, 2018; Sampson et al., 2018; Wellman, Coad, Flynn, Siam, & McLellan, 2019), among other sports. The primary emphases of many of these investigations were to establish field-based validity (Delaney et al., 2019; Kyprianou et al., 2019; Roe et al., 2017; Roell, Roecker, Gehring, Mahler, & Gollhofer, 2018) and reliability (Luteberget et al., 2018; Thornton, Nelson, Delaney, Serpiello, & Duthie, 2019; Van Iterson et al., 2017) of several Optimeye S5 measures. The most common of these measures is PlayerLoad™, an accelerometer-derived variable which is calculated as a scaled vector magnitude representing changes in triaxial acceleration (Barrett, Midgley, & Lovell, 2014).

PlayerLoad™ was first defined in the sports science literature approximately 10 years ago (Boyd, Ball, & Aughey, 2011; Montgomery, Pyne, & Minahan, 2010) and is quantified in terms of arbitrary units (i.e., units do not materially matter). PlayerLoad™ has been used widely

across a number of sports (McNamara, Gabbett, Chapman, Naughton, & Farhart, 2015; Schelling & Torres, 2016; Wik, Luteberget, & Spencer, 2017; Young, Gastin, Sanders, Mackey, & Dwyer, 2016); however, the metric's true formulation remains problematically opaque (Bredt, Chagas, Peixoto, Menzel, & de Andrade, 2020). Moreover, it remains unclear how PlayerLoad™ is associated with common IMU-based measures (e.g., vector magnitude activity counts, Euclidean norm minus one, etc.) for quantifying human movement more typically utilized in physical activity-related and biomechanical research.

**Problem Statement**

The *objective* of this study was to evaluate the associations of the PlayerLoad™ metric with common IMU-based physical activity-related and biomechanical measures of human movement including vector magnitude activity counts (VM), band pass filtered Euclidean norm (BFEN), and the Euclidean norm minus one (ENMO). The *central hypothesis* was that PlayerLoad™ would be strongly associated with VM, BFEN, and ENMO.

**Specific Aims and Hypotheses**

**Aim #1.** To quantify, evaluate, and compare the associations for PlayerLoad™ with VM, BFEN, and ENMO under simulated free-living conditions using publicly available IMU data.

***Hypothesis specific to aim #1.*** Our primary hypothesis was that the PlayerLoad™ metric would be strongly associated with VM, BFEN, and ENMO under a variety of simulated free-living conditions and at multiple measurement locations on the body.

**Aim #2**. To develop models for predicting PlayerLoad™ from BFEN and ENMO using publicly available IMU data representing human movement during numerous simulated free-living conditions.

***Hypothesis specific to aim #2.*** Our secondary hypothesis was that generalizable models with limited over-optimism would be developed for predicting PlayerLoad™ from BFEN and ENMO.

## Assumptions and Limitations

**Assumptions.** The publicly available IMU data we used to evaluate the associations between PlayerLoad™ and VM, BFEN, and ENMO were not collected using any monitoring device manufactured by Catapult – the company whose products typically provide estimates of PlayerLoad™. As such, in order to generalize our results, we assume some level of comparability between measurements from the IMU sensors within the publicly available data we analyzed and that which can be obtained directly from Catapult devices. Available evidence suggests that derived metrics from different IMU sensors or accelerometers compare reasonably well (Rowlands et al., 2018). However, some caution regarding the interchangeability of predictive models using data from different IMU sensors or accelerometers should be considered.

**Limitations.** As this investigation entailed analyses of publicly available IMU data, we were unable to select the specific modes and durations of activity best suited for developing robust and validated models for predicting PlayerLoad™. Additionally, available publications and presentations associated with these publicly available IMU data provide scant details regarding the descriptive characteristics of study participants. As such, our limited understanding of the participants who took part in these studies tempers our ability to strongly generalize beyond our sample.

## Definition of Terms

The following list contains operationalized definitions for numerous terms used herein:

- *Acceleration*
    - Acceleration is defined as change in velocity with respect to time. As a quantity, acceleration is usually standardized in terms of gravitational units (*g*; 1 $g$ = 9.8 $m \cdot s^{-2}$). Because acceleration is proportional to the net external force involved during movement, and as such more directly reflective of energy costs, measuring physical activity using acceleration is preferred to using speed (Chen & Bassett, 2005).
- *Accelerometer*
    - A sensor that measures proper acceleration along reference axes (Chen & Bassett, 2005). When attached to a participant's body, if the participant is at rest, the accelerometer measures the participant's orientation relative to the gravitational vector. If the participant is moving, the accelerometer measures a combination of the participant's acceleration and orientation (Xiao et al., 2016).
- *Accelerometry*
    - The collection of accelerometer data for deriving velocity and displacement information by integrating accelerometer data with respect to a given time interval (Chen & Bassett, 2005).
- *Band Pass Filtered Euclidean Norm (BFEN)*
    - This is a summary acceleration metric used in physical activity-related research created by band pass filtering triaxial acceleration signals (typically via an infinite-impulse response filter) and then quantifying the Euclidean norm from the post-filtered signals (van Hees et al., 2014).

- *Euclidean Norm Minus One (ENMO)*
    - This is a summary acceleration metric used in physical activity-related research created by quantifying the Euclidean norm from triaxial acceleration signals and subtracting 1 (van Hees et al., 2014).
- *Global Navigation Satellite System (GLONASS)*
    - A global satellite and positioning system developed by the Soviet Union during the 1970s. Commercial navigation using GLONASS was not possible until 2007 when the first GLONASS navigation device was introduced. Currently the system is powered by a constellation of 24 operational satellites (NovAtel Inc., 2020).
- *Global Navigation Satellite System (GNSS)*
    - A constellation of satellites which provide space-based position and timing signals with global coverage. Examples of GNSS include Russia's Global Navigation Satellite System (GLONASS) and the United States of America's Global Positioning System (GPS; European Global Navigation Satellite Systems Agency, 2020).
- *Global Positioning System (GPS)*
    - A global satellite-based radionavigation system belonging to the United States of America and operated by the United States Space Force. GPS was developed during the 1970s and achieved full operational capabilities in 1993. Commercial navigation using GPS was not possible until 1988 with the introduction of the first GPS navigation device. Currently the system is powered by a constellation of 31

operational satellites (United States Department of Defense, 2008; United States Space Force, 2020).

- *Gyroscope*
    - A device or sensor used for maintaining or measuring angular velocity and orientation. Structurally, a gyroscope contains a spinning wheel or disc where the axis of rotation is free to assume any orientation. Due to the conservation of angular momentum, while rotating, the orientation of the axis of rotation is unaffected by tilting or rotation of the mounting (Kabai, 2007).
- *Inertial Measurement Unit (IMU)*
    - A combined measurement system which integrates multiple inertial sensors. Typical sensors integrated into an IMU include an accelerometer, gyroscope, and magnetometer. In modern applications, the IMU's inertial sensors are typically integrated as a micro-electromechanical system (MEMS; Starlino Electronics, 2009).
- *Magnetometers*
    - A device or sensor used to measure magnetic field intensity (magnetic induction). Magnetometers can be used to measure geomagnetic field vector information to assist in providing estimates of position and orientation (You, 2017).
- *PlayerLoad*™
    - A trademarked name associated with a proprietary measure produced by the Catapult series of performance assessment devices. PlayerLoad™ is generally defined as the sum of acceleration changes over a given epoch across all three

accelerometer axes. This quantity accounts for instantaneous rate of acceleration change and divides it by a scaling factor of 100 (Julien, 2019).

- *Proper Acceleration*
    - Proper acceleration is the physical acceleration (i.e., measurable acceleration) experienced by an object (Taylor & Wheeler, 1992).
- *Vector Magnitude Low-Frequency Extension Activity Counts (VMLFE)*
    - This is a proprietary summary measure produced by ActiGraph products and calculated from the combined magnitude of triaxial activity counts using the 3-dimensional representation of the Pythagorean theorem. Low-frequency extension activity counts refer to those calculated using a more sensitive filtering algorithm and as such are typically greater in absolute magnitude than normal filter activity counts (Cain, Conway, Adams, Husak, & Sallis, 2013).
- *Vector Magnitude Normal Filter Activity Counts (VMNF)*
    - This is a proprietary summary measure produced by ActiGraph products and calculated from the combined magnitude of triaxial activity counts using the 3-dimensional representation of the Pythagorean theorem. The normal filter activity counts refer to those calculated using a less sensitive filtering algorithm and as such are typically smaller in absolute magnitude than low-frequency extension activity counts (Cain et al., 2013).

# Chapter 2. Review of Literature

## Background

Over the last 40 years, numerous wearable technologies have been introduced to quantify human movement. Examples of such technologies include pedometers to measure stepping (Bassett & Strath, 2002), cycle-based meters to measure power output (Bini, Diefenthaeler, & Carpes, 2014; Passfield et al., 2017), and accelerometers to measure physical activity and workloads (Sasaki, da Silva, Gonçalves Galdino da Costa, & John, 2016). More recently, there has been increasing interest in measuring and quantifying human movement in athletic contexts (Camomilla et al., 2018). Wearable technologies provide unique opportunities to objectively measure athletes and their movements. Sport-based wearable devices can measure variables such as top speed attained during a practice, the number of times an athlete changes direction in a given time frame, and total distance covered, among many other variables which could be quantified (Camomilla et al., 2018). For sport recruiters and scouts, data from these wearable technologies can be used to monitor the performance of athletes in order to facilitate peer-to-peer comparisons. For coaches and trainers, this data may indicate areas of performance that need improvement via practice adjustments or training modifications. Moreover, training adjustments utilizing this data may help to reduce the risk of injury (Luteberget et al., 2018).

Despite the rapid adoption and uptake of wearable devices by sport practitioners and coaches, the technologies underlying the development of these devices largely emanated out of several public health-related fields. This review will focus on 1) the evolution of several common wearable technologies now used to measure athletic performance, and 2) the PlayerLoad™ metric, introduced by Catapult Group International Ltd., for quantifying the dosage of physical movement over a set time interval.

## Common Wearable Technologies in Athletics

Modern wearable devices are typified by an amalgam of measurement sensors integrated into a single assessment system (Ainsworth, Cahalin, Buman, & Ross, 2015). Common technologies found in modern wearables include heart rate monitors, GPS, accelerometers, gyroscopes, and magnetometers. Below we will explore the evolution of the three former and most prevalent assessment technologies while also focusing on their typical applications.

### Heart Rate Monitors

The relationships between heart rate and physical exercise have been extensively studied in the fields of kinesiology and exercise science. Heart rate, in its most simplistic sense, refers to the number of times the heart beats during a specified time interval. Most commonly, heart rate is quantified in terms of beats per minute (bpm). In general, heart rate increases as the intensity of physical activity increases. For steady state exercise, this increase generally follows a linear pattern throughout the majority of the intensity spectrum (Åstrand, Rodahl, Dahl, & Strømme, 2003). However, during non-steady state activities the relationship between heart rate and oxygen uptake (i.e., energy expenditure) weakens and may not demonstrate a significant linear trend (Bot & Hollander, 2000).

The primary method for measuring heart rate is via electrocardiography (ECG or EKG). This method measures the electrical activity of the heart. Traditionally, this electrical activity is mapped in time to depict the heart's electrical wave form. The heart's electrical wave form is typically divided into a series of landmarks which represent several distinct phases of the heart's functioning. Examples include the P wave indicative of atrial depolarization, the QRS complex representing ventricular depolarization, and the T wave representing ventricular repolarization. In clinical settings the primary ECG measurement method is the 12 lead ECG (Jahrsdoerfer,

Giuliano, & Stephens, 2005). In contrast, wearable devices monitoring heart rate include chest straps utilizing ECG technology and wrist-based measurements utilizing an unrelated technology known as photophlethysmography (PPG; Zhang, Pi, & Liu, 2015).

Embedded sensors in an ECG-based chest strap allow for detection of the heart's electrical impulses (Leger & Thivierge, 1988). These impulses are then transmitted to a receiver unit, often worn on the wrist, which internally calculates the time-based location of each heartbeat. Through dimensional analysis these electrical signals are often converted into the metric of bpm which allows for the monitoring of physical activity intensity. ECG-based chest straps typically have an error rate of less than 5 bpm and are considered accurate for most purposes (Terbizan, Dolezal, & Albano, 2002).

Unlike ECG-based methods, PPG uses a light source to illuminate bodily tissues at or very near the skin's surface (Tamura, Maeda, Sekine, & Yoshida, 2014). A paired photodetector measures variation in the reflected light intensity which is associated with changes in the blood flow volume of local tissue. The changes in light intensity measured by the photodetector can then be mapped over time with peaks typically succeeding QRS complexes from a traditional ECG. Although this measurement method is primarily employed at the wrist, there are PPG devices available for measuring heart rate at alternative locations (e.g., forearm). Current evidence suggests that PPG-based devices are less accurate than ECG-based chest straps with error rates approaching 10 bpm (or higher) for some activities (Benedetto et al., 2018; Wallen, Gomersall, Keating, Wisloff, & Coombes, 2016).

For both ECG- and PPG-based heart rate monitors, the most typical usage is to track heart rate for monitoring intensity of activity during aerobic exercise. Commonly, heart rate is tracked using these devices to ensure training conforms to preidentified ranges of heart rate

maximum or heart rate reserve (American College of Sports Medicine, 2018). Additionally, other techniques exist to directly translate measured heart rate to additional outcomes such as energy expenditure (e.g., kcals/min; Keytel et al., 2005).

**GPS**

GPS technology was developed by the United States' Department of Defense in 1973 with the entirety of the original 24-satellite system operational in 1993. GPS represents one of the specific geo-spatial positioning systems referred to as a Global Navigation Satellite System (GNSS). Another prominent example of a GNSS is Russia's Global Navigation Satellite System (GLONASS). In both cases, these satellites (GPS and GLONASS) are able to determine location by way of trilateration between three or more of the rotating satellites (Rahman, 2012). Since GPS was made fully available to the public in 2000, the technology has been embedded in many commercial and household devices. One of the first studies to investigate GPS technology for potential future use in athletics was published in 1997 and found that the system could be used to monitor and evaluate human ambulation (Schutz & Chambaz, 1997). Within the next 10 to 15 years, more studies were conducted evaluating the reliability and validity of GPS technology (Coutts & Duffield, 2010; Jennings, Cormack, Coutts, Boyd, & Aughey, 2010). Expanding on this work, further published studies have monitored athletes in a variety of sports assessing variables such as speed or distance while also seeking to integrate GPS technology with data from other measurement devices such as accelerometers (Beato, Devereux, & Stiff, 2018; Buchheit, Gray, & Morin, 2015; Colby, Dawson, Heasman, Rogalski, & Gabbett, 2014).

As with any assessment technology, there are several limitations to GPS for measuring sport performance and free-living behavior. It is well understood that GPS capabilities are less reliable indoors away from a clear line of sight to the satellite(s) (Kuusniemi, Lachapelle, &

Takala, 2004). Moreover, since the majority of athletic events, practices, and free-living time is spent inside, the potential for GPS signal loss may be quite high in some circumstances.

Initial interest in using GPS to monitor physical activity centered around identifying locations where physical activity occurred (Troped, Wilson, Matthews, Cromley, & Melly, 2010). Concurrent with monitoring general physical activity, interest has grown in mapping routes of sport-related physical activity and exercise (Duncan, Badland, & Mummery, 2009; Jennings et al., 2010; Zhihua, 2008). Additionally, GPS technology is currently used to quantify speed of motion for activities such as running and cycling (Rampinini et al., 2015; Witte & Wilson, 2004).

**Accelerometers**

Accelerometry refers to a collection of assessment techniques attempting to measure acceleration most typically via electromechanical devices called accelerometers. Acceleration in this case is defined as change in velocity divided by change in time ($\Delta$Velocity / $\Delta$Time). Initial interest in monitoring human movement with accelerometers began in the middle of the 20$^{th}$ century with research evaluating the biomechanics of human movement (Cavagna, Saibene, & Margaria, 1961; Contini, Gage, & Drillis, 1965). Later during the 1970s and early 1980s, several studies attempting to distinguish between sleeping and wakefulness while wearing a wrist-based accelerometer were published (Kripke, Mullaney, Messin, & Wyborney, 1978; Mullaney, Kripke, & Messin, 1980). Shortly thereafter, a number of published reports began to examine using accelerometers as a physical activity measurement tool (Montoye et al., 1983; Servais, Webster, & Montoye, 1984; Wong, Webster, Montoye, & Washburn, 1981). Since this time, accelerometry as a means to assess physical activity has become commonplace, as evidenced by

the more than 70 PubMed articles containing the title words “physical activity” and “accelerometer” published during 2019.

Currently, most accelerometers used to quantify human movement are piezoelectric or capacitive devices which can detect acceleration along three orthogonal axes (vertical, mediolateral, and anteroposterior; John & Freedson, 2012). Acceleration is typically quantified in gravitational units by most devices whereby 1 g is equivalent to the acceleration due to gravity (9.81 $m/s^2$). Although speed or velocity as a measure of human performance may be more interpretable for describing bodily motion, it is less useful than acceleration when attempting to quantify the energy costs associated with activity (Chen & Bassett, 2005). This is because acceleration is proportional to the net external force involved and therefore more reflective of the energy costs associated with human movement.

Contemporary methods for utilizing an accelerometer to measure bodily acceleration include 1) calculation of so-called “activity counts” to quantify the total volume of physical activity over a user-specified time interval (Wolff-Hughes, Troiano, Boyer, Fitzhugh, & McClain, 2016), 2) estimation of time spent in various intensities of activity (e.g., sedentary, light, moderate, and vigorous) using threshold methods (Watson, Carlson, Carroll, & Fulton, 2014), and 3) prediction of physical activity type and energy expenditure using machine learning/artificial intelligence approaches (Staudenmayer, Pober, Crouter, Bassett, & Freedson, 2009). Common acceleration-based metrics utilized within the aforementioned methods for quantifying the dosage of physical movement over a specified time interval include activity counts, BFEN, and ENMO.

Accelerometer-determined activity counts is the most prevalent metric used to quantify time-based intensity of human movement via objective means in physical activity research.

There are a number of research-grade accelerometers which produce this metric (Straker & Campbell, 2012); however, activity counts are typically not comparable across different branded devices. Activity counts produced using ActiGraph products (ActiGraph, LLC., Pensacola, Florida) are most common as ActiGraph accelerometers are the most widely used research-grade devices within the published literature base (Leinonen et al., 2017). Activity counts are expressed as dimensionless units (Stone, Rowlands, & Eston, 2009); however, higher absolute values of activity counts within a given time interval are indicative of higher intensities of physical activity or movement (Freedson, Melanson, & Sirard, 1998). Activity counts measured at various body locations consistently demonstrate positive associations with energy expenditure (Freedson et al., 1998; Swartz et al., 2000). However, ActiGraph activity counts specifically come in two different varieties 1) low-frequency extension (LFE) activity counts, and 2) normal filter (NF) activity counts. Generally speaking, for a given time interval with the same absolute level of physical activity intensity, the absolute magnitude of LFE activity counts will almost always be greater than NF activity counts (Cain et al., 2013). Activity counts are typically generated for all accelerometer axes (most typically triaxial today) as well for the combined VM.

In contrast to proprietary activity counts, common non-proprietary accelerometer measures for quantifying time-based human movement are BFEN and ENMO (van Hees et al., 2014; van Hees et al., 2013). BFEN is calculated by first band pass filtering each axis of raw acceleration data in g-units from a triaxial accelerometer using an infinite-impulse response filter. These filters are typically $4^{th}$ order Butterworth prototypes with -3 dB high pass cutoffs of 0.2-0.5 Hz and a low pass cutoff of 15 Hz (van Hees et al., 2014; van Loo et al., 2018). The post-filtered triaxial signals are then combined as the Euclidean norm via the 3-dimensional generalization of Pythagoras's theorem. This band pass filtering approach attenuates the power

spectrum of the underlying signal beyond the edges of the cutoff frequencies. In short, very low and high frequency components of the signal, indicative of non-human movement, are significantly attenuated. This also produces an estimated gravity-subtracted signal as the acceleration due to gravity is convolved with signal elements in the lower frequency range (van Hees et al., 2013). Unlike BFEN, ENMO does not require any filtering of the underlying acceleration signal. Instead, ENMO is calculated by combining the raw triaxial signals as the Euclidean norm and subtracting 1 (van Hees et al., 2013). As the Euclidean norm of an object equals 1 g (acceleration due to gravity) when at rest, it assumed that ENMO will equal 0 when an accelerometer is at rest. Unfortunately, it is rather common for research-grade physical activity accelerometers to drift slightly out of calibration over time (e.g., an accelerometer at rest will measure < or > 1 g), in which case the ENMO metric may yield negative estimates in some instances (van Hees et al., 2014). Units of measurement for BFEN and ENMO are typically expressed in milligravity units per second (mg/s) and both metrics are positively associated with energy expenditure when used to quantify human movement (Hibbing, Lamunion, Kaplan, & Crouter, 2018; Migueles et al., 2019).

**Multi-Sensor Sport Performance Devices**

Assessment systems for physical activity and exercise combining multiple measurement sensors are by no means novel. Early work in this research area focused on improving physical activity energy expenditure predictions using multiple sensor inputs. One early approach for improving physical activity energy expenditure estimates using wearable technology was realized with the Actiheart device (Brage, Brage, Franks, Ekelund, & Wareham, 2005). The Actiheart combines a small mobile ECG unit and accelerometer, both worn on the chest, and has been demonstrated to provide reasonably accurate (mean error = 0.005 kcals $\cdot$ kg$^{-1}$ $\cdot$ min$^{-1}$) and

reliable estimates of physical activity energy expenditure across a range of activities (Crouter, Churilla, & Bassett, 2008). Subsequent to the Actiheart's introduction, another multi-sensor device, specifically designed for estimating minute-by-minute energy expenditure, was the now defunct SenseWear Armband (SWA). The SWA combined an accelerometer along with heat flux, skin temperature, and galvanic skin response sensors (Johannsen et al., 2010). Using a proprietary algorithm, the SWA combined data from each of the sensor inputs to estimate real-time energy expenditure and was extensively studied at the time (Calabro, Welk, & Eisenmann, 2009; Drenowatz & Eisenmann, 2011; Johannsen et al., 2010; Unick et al., 2012).

More recently, several commercial entities have developed new lines of sport performance-oriented multi-sensor devices. Prominent examples are the line of multi-sensor systems developed and marketed by gpexe, STATSports, and Catapult Sports. The primary measurement sensors for each one of these devices are triaxial acceleromters, gyroscopes, and magnetometers with all three sensors integrated into a single IMU.

In respect to Catapult's primary contemporary measurement device, the Optimeye S5, parameters that can be measured include maximum and average speed, collisions, changes in direction, and left-right gait imbalances (Camomilla et al., 2018). Additionally, the Optimeye S5 also provides estimates of what Catapult has called PlayerLoad™. The PlayerLoad™ metric represents the total cumulative change of acceleration experienced by a participant over a specified time interval (Camomilla et al., 2018). When tracked by coaches and trainers, the PlayerLoad™ metric can assist the coach or trainer in monitoring practice and training sessions to ensure training volume and intensity can be modified quickly to suit the individual needs of each athlete. This data can be stored locally using Catapult AMS software and viewed at a later date to compare training sessions on a daily, monthly, or annual basis.

Currently, Catapult claims that more than 2,500 sport teams around the world employ their technologies to measure athletic performance (Catapult, 2019). Several multi-sensor devices are offered by Catapult including the Optimeye S5, Vector, ClearSky, and PlayerTek. The latter three devices have just been brought to market and not extensively evaluated or studied. The former device represents Catapult's most popular human movement measurement system capable of providing estimates for a whole variety of sport performance-related parameters. Enclosed in one catapult device, is a GPS unit, an accelerometer, a gyroscope, and a magnetometer. The catapult device can also interface with a standard chest strap heart rate monitor. The Optimeye S5 has been previously evaluated among athletes in rugby (Hulin et al., 2017; Roe et al., 2017), ice hockey (Van Iterson et al., 2017), handball (Luteberget et al., 2018), and American football (Govus et al., 2018; Li et al., 2020; Murray et al., 2018; Sampson et al., 2018; Wellman et al., 2019), among other sports. Primary emphases in many of these investigations have sought to establish field-based validity (Delaney et al., 2019; Kyprianou et al., 2019; Roe et al., 2017; Roell et al., 2018) and reliability (Luteberget et al., 2018; Thornton et al., 2019; Van Iterson et al., 2017) of several Optimeye S5 measures.

Of particular scientific interest in the area of sport performance, Catapult's PlayerLoad™ metric has been extensively studied (Barrett et al., 2016; Barron, Atkins, Edmundson, & Fewtrell, 2014; Bullock et al., 2019; McNamara et al., 2015; Nicolella, Torres-Ronda, Saylor, & Schelling, 2018; Wik et al., 2017). PlayerLoad™ is defined in terms of change of triaxial acceleration with respect to time and has previously been demonstrated to have excellent reliability (Intra-Class Correlations = 0.80 to 0.97) and is highly correlated with average heart rate and oxygen uptake ($r = 0.92$ to 0.98; Barrett et al., 2014). PlayerLoad™ is another metric similar to activity counts, BFEN, and ENMO intending to quantify the dosage of physical

movement over a specified time interval (i.e., the higher the PlayerLoad™ value in a given time interval the more movement that occurred).

Despite similarities between PlayerLoad™ and activity counts, BFEN, and ENMO – all acceleration-derived metrics used to describe human movement – no published investigations have examined the associations between these metrics. As these metrics represent the most accepted methods for quantifying dosage of physical movement over a specified time interval for sport performance (PlayerLoad™) and physical activity applications (activity counts, BFEN, and ENMO) using wearable devices, evaluating the associations between these measures is a logical starting point to better understand their interchangeability and comparative strengths and weaknesses.

# Chapter 3. Methods

## Data Source

To address this study's aims, we used publicly available secondary data from the REAListic sensor DISPlacement (REALDISP) and Mobile Health (MHEALTH) studies (Banos et al., 2012; Banos, Garcia, et al., 2014; Banos, Toth, Damas, Pomares, & Rojas, 2014; Banos et al., 2015). Prior to any data analysis, we submitted a protocol application to the Oregon State University Institutional Review Board (IRB) seeking to determine whether this study required IRB review. As this investigation utilized de-identified and non-sensitive secondary data, the IRB rendered a determination that the study did not qualify as human subjects research. Therefore, the IRB concluded that formal review of the proposed study and its protocol was not required (Appendix A).

## Datasets

**REALDISP.** The REALDISP study originally intended to evaluate different sensor placements on the body and the associated effects of such placements on activity recognition (Banos et al., 2012; Banos, Toth, et al., 2014). This was accomplished by comparing three different methods of device placement on the body. First, the standardized or "ideal placement" represented device placement in a location that was deemed optimal by the research team. Second, self-device placement ("self-placement") was performed by the participant while intending to represent real-world applications where individuals potentially lack specific knowledge regarding optimal placement locations for wearable sensors. Lastly, a "mutual-displacement" or intentional displacement was introduced to better understand how intentional mispositioning of sensors may degrade the usefulness of activity recognition when compared to

"ideal" sensor placement. For consistency in our proposed analyses, we only used sensor data collected using the standardized or "ideal" placements.

Seventeen participants (10 males, ages 22 to 37 years-old) took part in the study (Banos, Toth, et al., 2014). Participants were asked to complete 33 exercises in a cardio-fitness room. Exercises ranged from movements involving interaction with machines and equipment such as running or rowing which were performed for 1 minute each to jumping rope and lateral arm raises consisting of 20 consecutive repetitions. Research staff demonstrated each exercise immediately prior to when participants performed them; however, participants were instructed to freely perform the activities to the best of their ability. The entire sequence of exercises took approximately 15 to 20 minutes to complete and was preceded by a 30-minute preparation phase to ensure proper placement of the sensors and participant familiarization with the protocol.

During all activities, participants were outfitted with a set of nine Xsens IMUs (Xsens Technologies, Enschede, Netherlands) placed at the 1) back – secured between the scapulae, 2) left calf – secured on the tibia halfway between the ankle and knee, 3) left lower-arm – secured at the mid-point of the forearm, 4) left thigh – secured on the anterior of the thigh at the midpoint of the femur, 5) left upper-arm – secured at the midpoint of the humerus, 6) right calf, 7) right lower-arm, 8) right thigh, and 9) right upper-arm (Banos, Toth, et al., 2014). Each IMU was hard-wired to an Xsens Master processing unit which streamed data wirelessly via Bluetooth in real-time to a dedicated laptop. The laptop was simultaneously used to associate timestamps with the performed activities and a redundant video recording was reviewed post-testing to correct any timestamp labeling mistakes. All IMUs collected triaxial acceleration, magnetometer, and gyroscope data at a sampling frequency of 50 Hz. For the "ideal" placement data, the average participant provided 13.0 ± 5.3 minutes of activity-related data.

**MHEALTH.** The MHEALTH study collected data from vital sign recordings and body motion-related movement sensors during a discrete set of physical activities (Banos, Garcia, et al., 2014; Banos et al., 2015). More broadly, the MHEALTH study aimed to develop an open-source Android-based implementation framework to facilitate rapid development of mHealth applications.

Ten participants of a diverse profile (no further descriptive information regarding the participants is presented in any published materials related to this study) performed a series of 12 physical activities including standing still, lying down, walking, jogging, and jumping front and back, among other activities (Banos et al., 2015). All activities were performed outside of a formal laboratory and no constraints were placed on the manner in which activities were to be executed; however, participants were encouraged to try their best when performing the activities.

During all activities, participants' bodily motion was captured in real-time using Shimmer2 (Shimmer Research Ltd., Dublin, Ireland) IMUs which were attached to the body via elastic straps and positioned at the 1) chest – over left pectoral muscle, 2) right wrist, and 3) left ankle. The IMUs collected triaxial acceleration, gyroscope, and magnetometer data. The chest-based IMU also had an integrated 2-lead ECG system for capturing electrical activity from the heart during all activities. All sensor data were collected at a sampling frequency of 50 Hz. All activity sessions were video-recorded and these recordings were used to complete post-protocol timestamp labeling of sensor data.

## Data Processing

REALDISP and MHEALTH data were downloaded freely from the publicly accessible University of California, Irvine – Machine Learning Repository (http://archive.ics.uci.edu). Downloaded raw triaxial acceleration data (50 Hz) from the REALDISP and MHEALTH studies

were resampled to 100 Hz to ensure greater compatibility in quantification methods for VMLFE, VMNF, BFEN, ENMO, and PlayerLoad™ metrics (Nicolella et al., 2018; van Hees et al., 2013). Resampling was accomplished by direct linear interpolation.

As acceleration data was collected in units of $m/s^2$, all data points were divided by 9.81 $m/s^2$ to yield additional data vectors in units of gravity (g). ActiLife software (version 6.13.4, ActiGraph, LLC., Pensacola, Florida) was used to create 1-second epochs of VMLFE and VMNF from the 100 Hz raw triaxial accelerometer data. Open-source metrics BFEN and ENMO, as well as PlayerLoad™, were computed using the raw 100 Hz triaxial accelerometer data and integrated to 1-second epochs.

On a sample-by-sample basis, BFEN was calculated by first band pass filtering the raw triaxial acceleration data (*x, y, z*) at 100 Hz using a 4th order Butterworth band pass filter with -3 dB cutoff frequencies of 0.2 and 15 Hz to yield filtered triaxial acceleration data ($x_f$, $y_f$, $z_f$). BFEN, in units of mg, was then calculated from the filtered triaxial accelerometer data as shown in Equation 1. In contrast to BFEN, ENMO does not require filtering of the input raw

$$BFEN = 1000 \times \sqrt{x_f^2 + y_f^2 + z_f^2} \qquad \text{(Equation 1)}$$

acceleration signals. ENMO combines the three triaxial vectors into a single measure in mg using the method displayed in Equation 2. Unlike BFEN and ENMO, PlayerLoad™ is calculated

$$ENMO = 1000 \times \left(\sqrt{x^2 + y^2 + z^2} - 1\right) \qquad \text{(Equation 2)}$$

from the absolute changes in raw triaxial acceleration from one sample (t-1) to the next sample (t). PlayerLoad™ was calculated in arbitrary units using the method displayed in Equation 3.

$$PlayerLoad™ = \sqrt{\frac{(x_t - x_{t-1})^2 + (y_t - y_{t-1})^2 + (z_t - z_{t-1})^2}{100}} \qquad \text{(Equation 3)}$$

All completed activities from the REALDISP data set were included in final analyses. However, we excluded all cycling-related data from the MHEALTH study resulting in an analytic data set containing acceleration information from only 11 activities. This was done because acceleration measures from the wrist are known to perform quite poorly in representing gross bodily movement during cycling (Welch et al., 2013). As such, we chose to eliminate cycling to prevent the activity from exerting disproportionate influence on subsequent association analyses and predictive modelling methods.

Two final analytic data files (.csv – one each for REALDISP and MHEALTH studies) containing time matched VMLFE, VMNF, BFEN, ENMO, and PlayerLoad™, with corresponding identifiers for participant, IMU location, and activity were created.

**Statistical Power**

As this was a secondary data analysis, potential statistical power for analytics were constrained to the structure and characteristics of the underlying data. We did, however, estimate post-hoc power for our primary analytic endpoints (i.e., PlayerLoad™ predictive models) using the smallest analytic sample of interest (110 observations) while accounting for the data's nested structure (multiple observations nested within 10 participants). Assuming a standard mixed-effects regression model with PlayerLoad™ regressed on another summary acceleration metric, an $\alpha$ level of 0.05, and a random intercept for participant, our least powerful analysis was able to achieve > 95% power to detect $R^2$ values $\geq 0.11$ – equivalent to a "medium" standardized effect size (Cohen, 1988).

**Statistical Analyses**

All analyses were conducted using R (version 3.6.2, R Foundation for Statistical Computing, Vienna, Austria) and the level of significance $\alpha$ was set at 0.05.

**REALDISP Analyses.** Means and standard deviations for VMLFE, VMNF, BFEN, ENMO, and PlayerLoad™ were initially computed for each combination of study participant, IMU location, and activity. Five separate two-way (IMU location × activity) linear mixed-effects models (equivalent to two-way within subjects repeated measures ANOVA) were fitted to evaluate mean differences in VMLFE, VMNF, BFEN, ENMO, and PlayerLoad™ across IMU locations (9 locations), performed activities (33 activities), and their interaction.

Trellis plots were then constructed to depict the bivariate relationships of PlayerLoad™ with VMLFE, VMNF, BFEN, and ENMO across the nine different IMU locations (Cleveland, 1993). To account for multiple observations per participant, repeated measures correlation coefficients were quantified using an ANCOVA framework (Bakdash & Marusich, 2017) for PlayerLoad™ vs. VMLFE, PlayerLoad™ vs. VMNF, PlayerLoad™ vs. BFEN, and PlayerLoad™ vs. ENMO across each of the nine IMU locations. Computed correlations within each of the four pairings were averaged across IMU locations using Fisher's z-transformation and its inverse to yield total average correlation coefficients. Correlation magnitudes between the nine IMU locations were compared using *z*-tests within the framework proposed by Silver, Hittner, and May (2004) for dependent nonoverlapping correlations. To control the familywise error rate among the 36 statistical comparisons within each correlation pairing, we employed a Bonferroni-correction by dividing our *a priori* $\alpha$ by 36 ($0.05 / 36 \rightarrow \alpha = 0.0014$). We also compared correlation magnitudes between the four pairings within each IMU location using Meng's *z*-test for dependent overlapping correlations (Meng, Rosenthal, & Rubin, 1992). A Bonferonni-correction was again used to control the familywise error rate among the 6 comparisons within each IMU location ($0.05 / 6 \rightarrow \alpha = 0.0083$).

Separate calibration models were then developed for predicting PlayerLoad™ estimated at the back IMU location using either BFEN or ENMO. To simplify model building, we used Tukey's Ladder of Powers method (Tukey, 1977) to perform two iterative searches identifying specific power transformations (-5 to 5 in 0.001 increments) for PlayerLoad™ that maximized linearity (i.e., maximized the correlation coefficient) with BFEN and ENMO. Linear mixed-effects models were then used to develop prediction equations for regressing power-transformed PlayerLoad™ separately on BFEN and ENMO. Model fit was assessed by quantifying pseudo $R^2$, root mean squared error (RMSE), and mean absolute error (MAE). Harrell's optimism bootstrap for predictive indices (Harrell, Lee, & Mark, 1996) was used to validate each model by estimating unbiased pseudo $R^2$, RMSE, and MAE using 10,000 bootstrap replicates.

**MHEALTH Analyses.** Means and standard deviations for BFEN, ENMO, and PlayerLoad™ were initially computed for each combination of study participant and activity. Three separate one-way (activity) linear mixed-effects models (equivalent to one-way within subjects repeated measures ANOVA) were fitted to evaluate mean differences in BFEN, ENMO, and PlayerLoad™ across performed activities (11 activities).

Scatterplots were then constructed to depict the bivariate relationships of PlayerLoad™ with BFEN and ENMO. To account for multiple observations per participant, repeated measures correlation coefficients were quantified for PlayerLoad™ vs. BFEN and PlayerLoad™ vs. ENMO. Correlation magnitudes between the two pairings were compared using Meng's *z*-test for dependent overlapping correlations.

Separate calibration models were then developed for predicting PlayerLoad™ estimated at the wrist using either BFEN or ENMO. To simplify model building, we used Tukey's Ladder of Powers method to perform two iterative searches identifying specific power transformations (-

5 to 5 in 0.001 increments) for PlayerLoad™ that maximized linearity (i.e., maximized the correlation coefficient) with BFEN and ENMO. Linear mixed-effects models were then used to develop prediction equations for regressing power-transformed PlayerLoad™ separately on BFEN and ENMO. Model fit was assessed by quantifying pseudo $R^2$, root mean squared error (RMSE), and mean absolute error (MAE). Harrell's optimism bootstrap for predictive indices was used to validate each model by estimating unbiased pseudo $R^2$, RMSE, and MAE using 10,000 bootstrap replicates.

# Chapter 4. Results

## REALDISP Analyses

In total, 2,451.5 minutes (147,090 seconds) of IMU data was collected from the study's 17 participants. When summarized to mean values for combinations of activity and IMU location, there was a total of 594 data points. Means, standard deviations, and ranges for VMLFE, VMNF, BFEN, ENMO, and PlayerLoad™ across all 594 combinations can be accessed online (shorturl.at/pIU45). A subset of these summary acceleration data illustrating several common activities as measured from the back-positioned IMU are depicted in Table 1.

**Table 1.** Acceleration values of selected activities measured via the back-positioned IMU.

| Activity | VMLFE<br>M ± SD<br>Min - Max | VMNF<br>M ± SD<br>Min - Max | BFEN<br>M ± SD<br>Min - Max | ENMO<br>M ± SD<br>Min - Max | PlayerLoad™<br>M ± SD<br>Min - Max |
|---|---|---|---|---|---|
| Walking | 51.2 ± 14.3<br>32.9 - 85.1 | 47.6 ± 15.3<br>27.1 - 83.4 | 164.6 ± 24.3<br>122.9 - 206.8 | 44.8 ± 8.1<br>30.7 - 66.4 | 35.8 ± 10.7<br>23.2 - 67.4 |
| Running | 156.7 ± 22.4<br>121.5 - 203.6 | 154.6 ± 22.5<br>119.2 - 201.8 | 839.5 ± 70.0<br>727.3 - 932.4 | 418.2 ± 45.6<br>350.1 - 496.3 | 268.5 ± 36.9<br>224.2 - 370.1 |
| Jumping Rope | 328.9 ± 32.1<br>266.6 - 382.6 | 328.0 ± 32.2<br>265.3 - 381.9 | 1118.0 ± 66.6<br>1033.8 - 1288.2 | 600.2 ± 42.0<br>548.3 - 720.9 | 257.8 ± 55.0<br>187.5 - 400.0 |
| Forward Stretching | 214.6 ± 56.9<br>129.4 - 357.6 | 213.3 ± 57.1<br>127.7 - 356.5 | 439.9 ± 109.1<br>290.8 - 716.1 | 158.5 ± 52.9<br>117.9 - 312.7 | 43.1 ± 13.3<br>31.5 - 79.1 |
| Heels to Butt | 225.7 ± 27.6<br>182.4 - 274.0 | 224.1 ± 27.7<br>180.7 - 273.1 | 1132.9 ± 82.8<br>1032.0 - 1364.5 | 572.9 ± 40.6<br>511.7 - 681.3 | 281.1 ± 60.5<br>191.4 - 395.3 |
| Rowing | 246.1 ± 45.8<br>156.4 - 312.7 | 245.1 ± 46.0<br>155.1 - 312.0 | 377.1 ± 77.6<br>240.5 - 497.3 | 66.8 ± 17.4<br>44.7 - 105.9 | 41.3 ± 11.3<br>25.1 - 69.5 |
| Cycling | 13.5 ± 13.7<br>1.9 - 50.8 | 9.6 ± 13.1<br>0.3 - 46.2 | 166.2 ± 84.0<br>58.8 - 375.5 | 52.4 ± 36.4<br>19.4 - 149.8 | 42.0 ± 24.6<br>11.2 - 102.3 |

***Note.*** VMLFE = vector magnitude low-frequency extension; VMNF = vector magnitude normal filter; BFEN = band pass filtered Euclidean norm; ENMO = Euclidean norm minus one. Units are in 1) activity counts/s for VMLFE and VMNF, 2) mg/s for BFEN and ENMO, and 3) PL/s × 100 for PlayerLoad™.

Two-way (location × activity) within-subjects linear mixed-effects models for VMLFE, VMNF, BFEN, ENMO, and PlayerLoad™ indicated highly significant effects for location, activity, and their interaction (location × activity; all $p < 0.001$).

Graphical depictions of the bivariate relationships of PlayerLoad™ with VMLFE and VMNF are depicted using Trellis plots in Figure 1. Both x- and y-axis scales are fixed across the

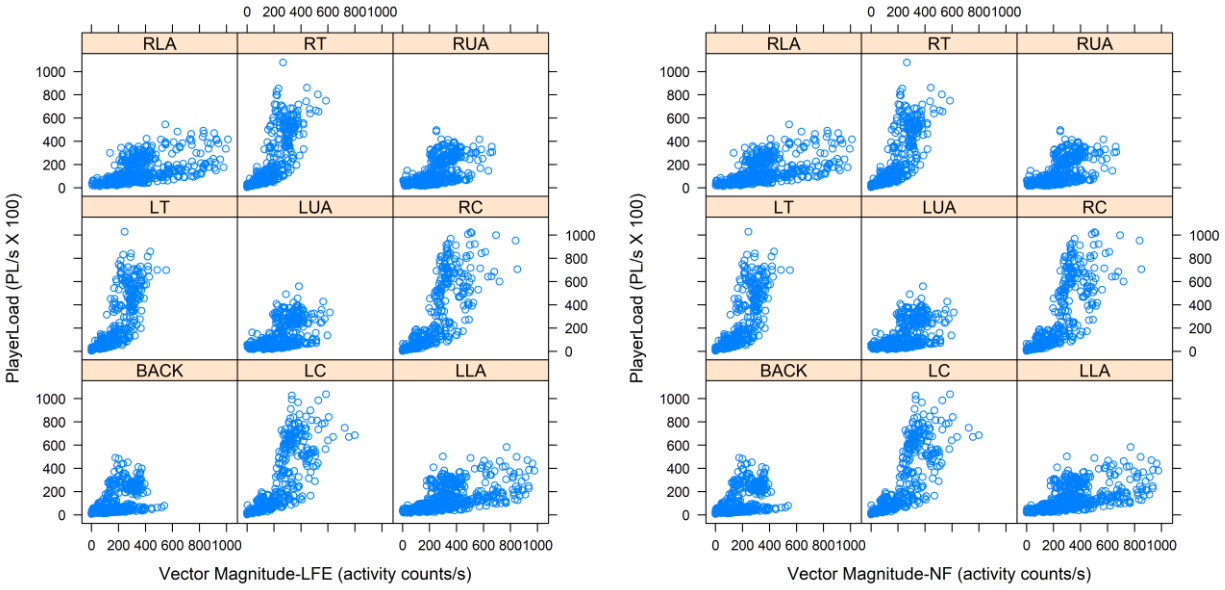


**Figure 1.** Trellis plots of relationships for PlayerLoad™ with Vector Magnitude Low-Frequency Extension (VMLFE) and Vector Magnitude Normal Filter (VMNF).

two figures and the general pattern of associations was similar for both VMLFE and VMNF. Linearity between PlayerLoad™ with VMLFE and VMNF was present with some heterogeneity in the shape of these relationships across IMU locations. Graphical depictions of the bivariate relationships of PlayerLoad™ with BFEN and ENMO are depicted using Trellis plots in Figure 2. Despite differences in the underlying quantifications of BFEN and ENMO, their visual relationships with PlayerLoad™ across IMU locations was similar. Again, linearity between

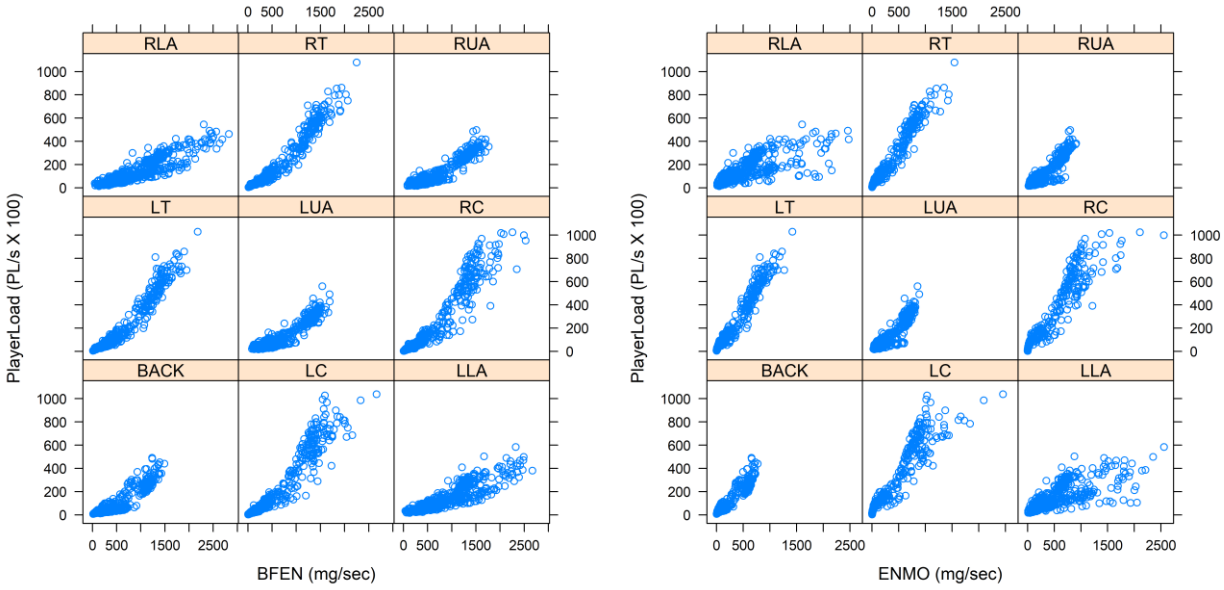


**Figure 2.** Trellis plots of relationships for PlayerLoad™ with Band Pass Filtered Euclidean Norm (BFEN) and Euclidean Norm Minus One (ENMO).

PlayerLoad™ with BFEN and ENMO was visibly evident with some heterogeneity in the depicted relationships across IMU locations. BFEN and ENMO appeared to visibly exhibit higher degrees of linearity with PlayerLoad™ than did either VMLFE or VMNF.

Correlation coefficients quantifying the magnitude of association for PlayerLoad™ with VMLFE, VMNF, BFEN, and ENMO are detailed in Table 2. Correlations for VMLFE and VMNF were nearly identical and always smaller than correlations associated with BFEN and ENMO. Across all nine IMU locations, BFEN and ENMO were strongly associated with PlayerLoad™ with nearly all correlations exceeding 0.80. For all evaluated metrics, measurements taken at lower-body IMU locations tended to be more strongly associated with PlayerLoad™ than did those taken on the upper-body. Average correlations across all nine IMU

**Table. 2** Correlation coefficients between summary acceleration metrics.

| IMU Location | VMLFE v. PlayerLoad™ | VMNF v. PlayerLoad™ | BFEN v. PlayerLoad™ | ENMO v. PlayerLoad™ |
|---|---|---|---|---|
| **Back** | $0.557^{a,1}$ | $0.556^{a,1}$ | $0.921^{ab,2}$ | $0.955^{a,3}$ |
| **LC** | $0.840^{b,1}$ | $0.840^{b,1}$ | $0.958^{c,2}$ | $0.951^{a,2}$ |
| **LLA** | $0.539^{a,1}$ | $0.539^{c,1}$ | $0.879^{d,2}$ | $0.742^{b,3}$ |
| **LT** | $0.827^{b,1}$ | $0.827^{b,1}$ | $0.974^{e,2}$ | $0.983^{c,3}$ |
| **LUA** | $0.569^{a,1}$ | $0.569^{a,2}$ | $0.936^{af,3}$ | $0.926^{d,4}$ |
| **RC** | $0.838^{b,1}$ | $0.838^{b,1}$ | $0.958^{c,2}$ | $0.951^{a,2}$ |
| **RLA** | $0.567^{a,1}$ | $0.567^{a,1}$ | $0.893^{b,2}$ | $0.764^{e,3}$ |
| **RT** | $0.830^{b,1}$ | $0.830^{b,1}$ | $0.975^{e,2}$ | $0.982^{c,3}$ |
| **RUA** | $0.580^{a,1}$ | $0.580^{a,2}$ | $0.939^{f,3}$ | $0.924^{d.4}$ |
| **Total** | $0.710^{1}$ | $0.710^{1}$ | $0.945^{2}$ | $0.938^{2}$ |

***Note.*** Values with different superscript letters within the same column are significantly different at 0.05/36 comparisons → $p < 0.0014$. Values with different superscript numbers within the same row are significantly different at 0.05/6 comparisons → $p < 0.0083$. VMLFE = Vector Magnitude Low Frequency Extension; VMNF = Vector Magnitude Normal Filter; BFEN = Band Pass Filtered Euclidean Norm; ENMO = Euclidean Norm Minus One. LC = left calf; LLA = left lower-arm; LT = left thigh; LUA = left upper-arm; RC = right calf; RLA = right lower-arm; RT = right thigh; RUA = right upper-arm.

locations for VMLFE and VMNF were not significantly different from each other (both $r$ = 0.710, $p$ = 0.361) nor were average correlations for BFEN and ENMO ($r$ = 0.945 vs. $r$ = 0.938, respectively, $p$ = 0.051). However, PlayerLoad™ correlations with BFEN and ENMO were significantly higher than correlations with VMLFE and VMNF (all $p < 0.001$).

As ENMO and BFEN were more strongly associated with PlayerLoad™, additional analyses were performed to build models for predicting PlayerLoad™ from BFEN and ENMO using IMU data collected from the back – the primary location where PlayerLoad™ would be measured in sport performance applications using devices from Catapult. To this end, we first conducted two iterative searches to identify exponent transformation values for PlayerLoad™ which maximized the correlation with BFEN and ENMO (Figure 3). Exponent values which

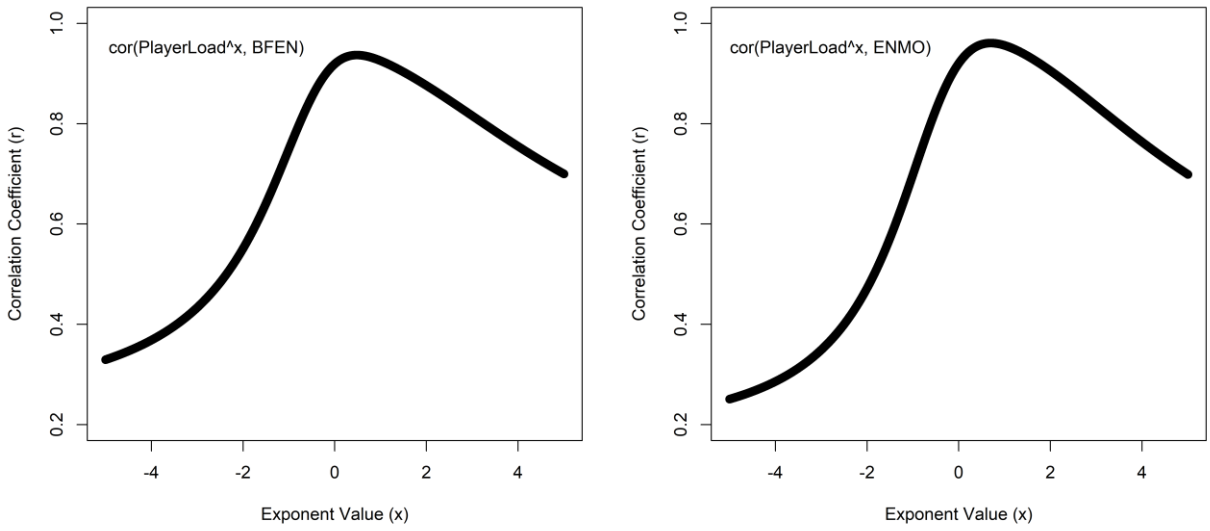


**Figure 3**. Plots depicting various PlayerLoad™ transformations and associated correlation coefficients for transformed PlayerLoad™ with Band Pass Filtered Euclidean Norm (BFEN; left) and Euclidean Norm Minus One (ENMO; right).

maximized correlation coefficients between PlayerLoad™ and BFEN ($x$ = 0.484) and ENMO ($x$ = 0.698) correspond to the peaks in the respective graphs within Figure 3.

Model calibration then followed by fitting linear-mixed effects models with transformed values of PlayerLoad™ regressed on BFEN and ENMO separately, and a random effect for participant. For BFEN and ENMO, models that included both random intercepts and slopes

performed better than intercept only models. As such, final models were fit with random intercepts and slopes. The final fixed-effects portions from the two models are depicted below in equations 4 and 5. Pseudo $R^2$ values were high (BFEN: $R^2 = 0.881$; ENMO: $R^2 = 0.930$) for both

$$PlayerLoad^{0.484} = BFEN \times 0.0011 + 0.3411 \quad \text{(Equation 4)}$$

$$PlayerLoad^{0.698} = ENMO \times 0.0029 + 0.3170 \quad \text{(Equation 5)}$$

models. Algebraic rearrangements of these two equations for predicting BFEN and ENMO from PlayerLoad™ can be found in Appendix B. Visual inspection of residual plots and histograms of residuals did not indicate clear evidence of heterogeneous variance or non-normality for BFEN or ENMO models. Bootstrap model validation results for BFEN and ENMO as sole fixed-effects predictors are depicted in Table 3. For PlayerLoad™ predicted by BFEN, optimism estimates were relatively small and in all instances the 95% confidence interval contained 0. Unbiased estimates (corrected index) for pseudo $R^2$, RMSE, and MAE deviated only slightly from the original model indices and do not indicate evidence of overfitting. Similarly, the model predicting PlayerLoad™ from ENMO yielded small optimism estimates with 95% confidence intervals for pseudo $R^2$ and MAE containing 0; however, some evidence of model over-optimism for RMSE estimates was observed as the 95% confidence interval did not contain 0. Still, unbiased estimates for pseudo $R^2$, RMSE, and MAE were only slightly higher than original model indices and are not suggestive of substantial model overfitting.

**MHEALTH Analyses**

In total, 405 minutes (24,300 seconds) of data was collected from the study's 10 participants wearing a wrist-mounted IMU. Means, standard deviations, and ranges for BFEN, ENMO, and PlayerLoad™ across 11 activities are presented in Table 4. One-way within-subjects

**Table 3.** Bootstrap validation results for REALDISP models predicting PlayerLoad™.

| Variables | Original Index | Training | Test | Optimism | Corrected Index |
|---|---|---|---|---|---|
| **BFEN** | | | | | |
| **$R^2$** | 0.881 | 0.883 | 0.881 | 0.002 (-0.012 – 0.015) | 0.879 |
| **RMSE** | 0.157 | 0.153 | 0.164 | -0.011 (-0.026 – 0.003) | 0.168 |
| **MAE** | 0.118 | 0.115 | 0.125 | -0.010 (-0.023 – 0.003) | 0.128 |
| **ENMO** | | | | | |
| **$R^2$** | 0.930 | 0.933 | 0.932 | 0.001 (-0.007 – 0.009) | 0.929 |
| **RMSE** | 0.175 | 0.169 | 0.192 | -0.023 (-0.045 – -0.004) | 0.198 |
| **MAE** | 0.127 | 0.122 | 0.136 | -0.014 (-0.028 – 0.001) | 0.140 |

***Note***. All values are presented as index estimates except for optimism which is presented as an index estimate and 95% confidence interval (obtained via percentile bootstrap). $R^2$ = pseudo r-squared; RMSE = root mean squared error; MAE = mean absolute error.

linear mixed-effects models for BFEN, ENMO, and PlayerLoad™ indicated highly significant main effects for activity in each model (all $p < 0.001$).

Graphical depictions of the bivariate relationships of PlayerLoad™ with BFEN and ENMO are presented using scatterplots in Figure 4. Relationships for PlayerLoad™ with BFEN and ENMO demonstrated similar patterns of linearity. Correlations for PlayerLoad™ with BFEN ($r = 0.955$) and ENMO ($r = 0.960$) were strong and not significantly different ($p = 0.560$).

To inform model development, two iterative searches were conducted to identify exponent transformation values for PlayerLoad™ which maximized the correlation coefficients with BFEN and ENMO when measured at the wrist (Figure 5). Exponent values which maximized correlation coefficients for PlayerLoad™ with BFEN ($x = 0.590$) and ENMO ($x =$

**Table 4.** Acceleration values of various activities measured via a wrist-positioned IMU.

| Activity | BFEN<br>M ± SD<br>Min - Max | ENMO<br>M ± SD<br>Min - Max | PlayerLoad™<br>M ± SD<br>Min - Max |
|---|---|---|---|
| Standing Still | 16.5 ± 4.0<br>13.2 - 26.3 | 2.5 ± 1.8<br>0.6 - 6.0 | 12.3 ± 0.9<br>11.1 - 13.8 |
| Sitting and Relaxing | 13.4 ± 1.0<br>11.9 - 15.7 | 1.2 ± 0.7<br>0.0 - 2.4 | 12.4 ± 0.9<br>11.4 - 14.0 |
| Lying Down | 13.7 ± 1.9<br>11.8 - 17.1 | 5.4 ± 5.3<br>0.4 - 14.8 | 12.3 ± 0.9<br>11.3 - 14.2 |
| Walking | 242.0 ± 36.8<br>184.0 - 315.3 | 111.8 ± 29.1<br>72.5 - 170.9 | 47.2 ± 11.0<br>34.5 - 68.9 |
| Climbing Stairs | 246.2 ± 52.8<br>178.5 - 334.6 | 85.3 ± 22.1<br>58.0 - 128.1 | 35.2 ± 6.9<br>24.8 - 48.7 |
| Waist Bends Forward | 267.7 ± 56.9<br>192.8 - 344.5 | 92.7 ± 30.3<br>53.8 - 148.3 | 39.1 ± 11.3<br>24.4 - 61.6 |
| Front Arm Elevations | 755.2 ± 94.1<br>633.0 - 905.5 | 130.0 ± 34.8<br>73.7 - 207.3 | 48.8 ± 14.2<br>33.1 - 76.2 |
| Crouching Knee Bends | 256.8 ± 49.2<br>192.7 - 334.3 | 90.9 ± 24.6<br>67.1 - 133.6 | 41.9 ± 10.7<br>27.8 - 61.5 |
| Jogging | 1237.1 ± 156.1<br>976.9 - 1540.1 | 539.8 ± 109.6<br>382.3 - 746.2 | 209.5 ± 24.9<br>174.1 - 248.2 |
| Running | 1651.1 ± 198.4<br>1307.8 - 2048.2 | 900.0 ± 202.7<br>557.2 - 1288.6 | 274.7 ± 26.3<br>238.8 - 316.1 |
| Jumping Front/Back | 1188.8 ± 165.8<br>950.8 - 1476.5 | 505.0 ± 125.7<br>321.3 - 755.4 | 238.6 ± 39.6<br>179.7 - 296.5 |

***Note.*** BFEN = Band pass filtered Euclidean norm; ENMO = Euclidean norm minus one. Units are in 1) mg/sec for BFEN and ENMO, and 2) cg/sec for PlayerLoad™.

1.636) correspond to the peaks in the respective graphs within Figure 5. Model calibration then followed by fitting linear-mixed effects models with transformed values of PlayerLoad™ regressed on BFEN and ENMO separately, and a random effect for participant. For BFEN, the model that included both a random intercept and slope did not perform better than the intercept

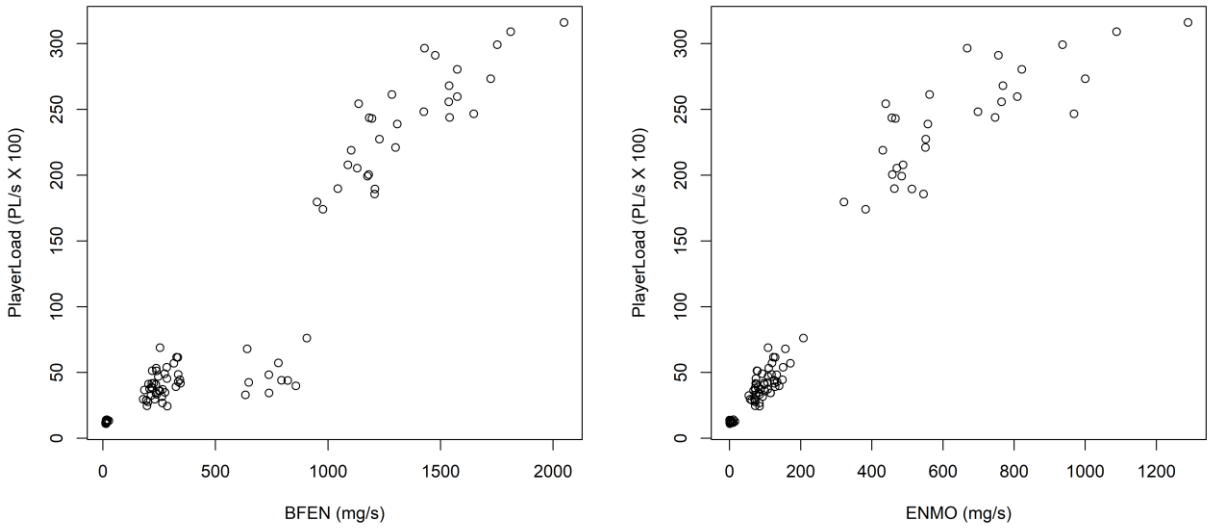


**Figure 4.** Scatterplots of relationships for PlayerLoad™ with Band Pass Filtered Euclidean Norm (BFEN) and Euclidean Norm Minus One (ENMO).

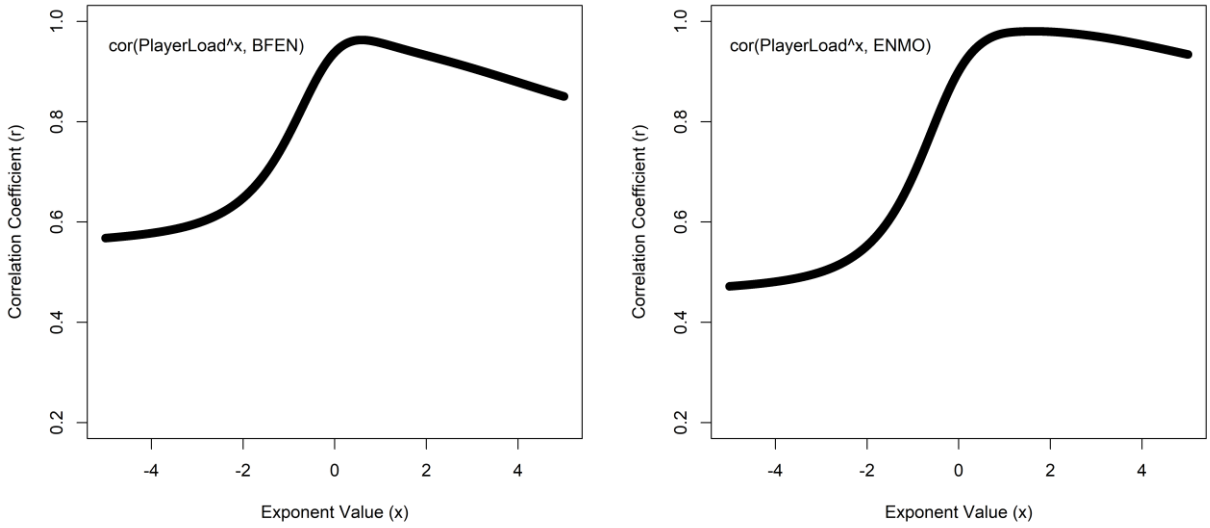


**Figure 5.** Plots depicting various PlayerLoad™ transformations and associated correlation coefficients for transformed PlayerLoad™ with Band Pass Filtered Euclidean Norm (BFEN; left) and Euclidean Norm Minus One (ENMO; right).

only model. For ENMO, the model that included both a random intercept and slope performed best. As such, final models were fit with a random intercept only for BFEN and a random intercept and slope for ENMO. The final fixed-effects portions from the models are depicted in equations 5 and 6. Pseudo $R^2$ values were high (BFEN: $R^2 = 0.921$; ENMO $R^2 = 0.932$).

$$PlayerLoad^{0.590} = BFEN \times 0.0010 + 0.2969 \quad \text{(Equation 5)}$$

$$PlayerLoad^{1.636} = ENMO \times 0.0065 - 0.1561 \quad \text{(Equation 6)}$$

Algebraic rearrangements of these two equations for predicting BFEN and ENMO from PlayerLoad™ can be found in Appendix B. Visual inspection of residual plots and histograms of residuals did not indicate clear evidence of heterogeneous variance or non-normality for BFEN or ENMO models. Bootstrap model validation results for BFEN and ENMO as the sole predictor are depicted in Table 5. For PlayerLoad™ predicted by BFEN, optimism estimates were relatively small and in all instances the 95% confidence interval contained 0. Unbiased estimates for pseudo $R^2$, RMSE, and MAE deviated only slightly from the original model indices and do not indicate evidence of overfitting. Similarly, the model predicting PlayerLoad™ from ENMO yielded small optimism estimates with 95% confidence intervals for pseudo $R^2$, RMSE, and MAE all containing 0. Unbiased estimates for pseudo $R^2$, RMSE, and MAE were only slightly higher than original model indices and are not suggestive of substantial model overfitting.

**Table 5.** Bootstrap validation results for MHEALTH models predicting PlayerLoad™.

| Variables | Original Index | Training | Test | Optimism | Corrected Index |
|---|---|---|---|---|---|
| **BFEN** | | | | | |
| **$R^2$** | 0.921 | 0.921 | 0.923 | -0.002 (-0.023 – 0.015) | 0.923 |
| **RMSE** | 0.155 | 0.151 | 0.157 | -0.006 (-0.041 – 0.025) | 0.161 |
| **MAE** | 0.102 | 0.099 | 0.103 | -0.004 (-0.028 – 0.021) | 0.106 |
| **ENMO** | | | | | |
| **$R^2$** | 0.932 | 0.943 | 0.931 | 0.012 (-0.012 – 0.039) | 0.920 |
| **RMSE** | 0.470 | 0.439 | 0.528 | -0.089 (-0.226 – 0.033) | 0.558 |
| **MAE** | 0.314 | 0.296 | 0.353 | -0.058 (-0.133 – 0.025) | 0.372 |

***Note***. All values are presented as index estimates except for optimism which is presented as an index estimate and 95% confidence interval (obtained via percentile bootstrap). $R^2$ = pseudo r-squared; RMSE = root mean squared error; MAE = mean absolute error.

# Chapter 5. Discussion

The primary aim of this study was to quantify, evaluate, and compare the associations for PlayerLoad™ with VM activity counts (VMLFE and VMNF), BFEN, and ENMO under simulated free-living conditions using publicly available IMU data. We also developed a series of models for predicting PlayerLoad™ from BFEN and ENMO (and vice-versa) again using publicly available IMU data corresponding to a variety of simulated free-living activities.

Summary estimates of mean values significantly differed across IMU locations and activities in all analyses. Notable scale differences were evident as well between metrics with BFEN estimates exceeding 1,000 mg/sec while associated PlayerLoad™ estimates were often less than 50 PL/s × 100. Pertaining to the primary aim, our analyses supported our hypothesis as PlayerLoad™ was strongly associated with VMLFE, VMNF, BFEN, and ENMO. However, observed associations did statistically differ across IMU measurement locations. Additionally, associations between acceleration metrics computed from IMU sensors placed on the lower-body generally were of a greater magnitude than those placed on the upper-body. Additionally, PlayerLoad™ associations with BFEN and ENMO were consistently of a significantly greater magnitude than associations with VMLFE and VMNF.

In reference to the secondary aim, we were able to develop generalizable models for quantifying PlayerLoad™ from back- and wrist-positioned IMUs using BFEN and ENMO as sole predictors. We also algebraically rearranged each of these models to predict BFEN and ENMO from PlayerLoad™ when measured at both the back and wrist. Unbiased estimates of pseudo $R^2$ were > 0.878 for all models predicting PlayerLoad™ demonstrating strong predictive ability. Model validation analyses using the bootstrap did not indicate large over-optimism (suggestive of model overfitting) for pseudo $R^2$, RMSE, or MAE in any evaluated model.

ActiGraph activity counts-based metrics including VMLFE and VMNF demonstrated lower magnitudes of association with PlayerLoad™ ($r$ = 0.539 to 0.840) than the other evaluated metrics. This may be due to the aggressive band pass filtering used when generating ActiGraph activity accounts (John, Miller, Kozey-Keadle, Caldwell, & Freedson, 2012). The band pass filter used by ActiGraph has -3 dB cutoffs of approximately 0.13-0.29 Hz and 1.63-2.73 Hz (Brønd, Andersen, & Arvidsson, 2017; John et al., 2012; Peach, Van Hoomissen, & Callender, 2014). Raw acceleration signal power at each of these cutoffs will be attenuated 50% with dramatically greater attenuation occurring beyond this frequency range. In comparison, the same acceleration signal was used to produce PlayerLoad™; however, no filtering of the raw triaxial data occurred with this method.

In contrast to activity counts, BFEN and ENMO were more strongly associated with PlayerLoad™ ($r$ = 0.742 to 0.983) than VMLFE or VMNF. This is likely due to the smaller degree of signal processing used to generate BFEN and ENMO (van Hees et al., 2013; van Loo et al., 2018). The triaxial acceleration signals used to compute BFEN are band pass filtered before calculation of the Euclidean norm; however, the passband defined by the -3 dB cutoff frequencies is much larger with high pass cutoffs of 0.2-0.5 Hz and low pass cutoffs of 15 Hz. The post-filtered signal then maintains more signal power from the raw signal than does the post-filtered signal produced when computing VMLFE or VMNF in most instances. Conversely, ENMO uses no filtering process and simply calculates the Euclidean norm from triaxial accelerometer signals and subtracts 1 g associated with gravity (van Hees et al., 2013). ENMO is sensitive to the calibration status of the accelerometer (van Hees et al., 2014). A reliable post-hoc method is available to calibrate triaxial acceleration data prior to the calculation of ENMO; however, multiple days of free-living accelerometer data are typically required to use this

method. Ultimately, ENMO-based accelerometer measurements do have the potential to suffer from additional measurement error and reduced reliability due to the devices being out of calibration.

Pertaining to our analytical methods, the iterative linearization method we used to identify power-based transformations for PlayerLoad™ that maximized correlations with BFEN and ENMO allowed us to develop linear prediction models with a single fixed-effects predictor. We did explore using polynomial and piecewise regression methods to initially model the available data. However, practically speaking, the linearization transformation method was more straightforward, yielded less complex fitted models, and would generally make overfitting less of a concern.

In terms of real-world application, the models we have developed can be used to predict PlayerLoad™ from BFEN and ENMO estimates. Additionally, when considering the relative strength of association between metrics, the algebraic rearrangements we present make it possible to predict BFEN and ENMO from PlayerLoad™ as well. In either case, these prediction methods will be of use when only epoch or summary level data are available (i.e., no raw acceleration data available to recompute the actual variables). Still, care must be taken to ensure the appropriate prediction models are being used as the associations for PlayerLoad™ with BFEN and ENMO did differ across measurement locations. Put another way, we do not recommend using our prediction models for estimating acceleration metrics obtained from IMUs or accelerometers positioned at other locations on the body (i.e., above right hip in-line with mid-axillary line, ankle, chest, etc.).

Several studies present cut-point ranges of BFEN (Schaefer, Nigg, Hill, Brink, & Browning, 2014; van Loo et al., 2018) and ENMO (Hildebrand, VT, Hansen, & Ekelund, 2014;

van Loo et al., 2018) that correspond to different intensities of physical activity. As a single illustrative example, using the BFEN wrist cut-points of 314 mg and 998 mg (lower-bounds for moderate- and vigorous-intensity activity, respectively) from Schaefer et al. (2014), estimated PlayerLoad™ predictions consistent with these cut-point values would be 41.7 and 145.8 PL/s × 100, respectively. Although not ideal, the approach we just presented can be used to translate across the metrics we have provided and serve as a potential viable option until needed studies using gold-standard measures of energy expenditure (e.g., indirect calorimetry) can be completed to properly calibrate PlayerLoad™ as a predictor of time-based absolute physical activity intensity. Indeed, PlayerLoad™ may be a desirable measure to use for quantifying time-based physical activity intensity as the most common definition of PlayerLoad™ is defined simply as the vector magnitude of changes in triaxial acceleration divided by 100 (Boyd et al., 2011). Unlike VMLFE, VMNF, or BFEN, PlayerLoad™ does not rely on any signal filtering and is likely more robust to accelerometer calibration errors than ENMO, both of which are desirable measurement properties that may prove to be fruitful.

Despite optimism regarding the usefulness of our PlayerLoad™ prediction models, a growing chorus of sports scientists remain skeptical of this metric's usefulness for quantifying time-based human movement (Bredt et al., 2020; Staunton, Wundersitz, Gordon, & Kingsley, 2017). Most of this skepticism centers around the trade named and proprietary nature of PlayerLoad™. Limited details pertaining to the actual computation of PlayerLoad™ has been provided to the public by Catapult Sports. This is perhaps why PlayerLoad™ has four distinct acceleration-related definitions within the sports performance literature (Aguiar, Botelho, Gonçalves, & Sampaio, 2013; Boyd et al., 2011; Casamichana, Castellano, & Dellal, 2013; Randers, Nielsen, Bangsbo, & Krustrup, 2014). That aside, research by Nicolella et al. (2018)

has demonstrated that the traditional PlayerLoad™ definition from Boyd et al. (2011) produces estimates yielding correlations > 0.999 and comparable mean estimates with proprietary Catapult PlayerLoad™ values generated from AMS software.

As will all studies, this study is not without limitations. The study detailed herein was a secondary analysis of publicly available IMU data from two separate studies. For both studies, details pertaining to demographics and anthropometrics of the study sample were scant. Moreover, we had no control in choosing the specific sets of activities completed by the participants nor did we have any control over the delivery of these activities for this protocol. It would have been beneficial to have larger participant samples that completed more activities for longer durations. However, although the REALDISP and MHEALTH data sets we used only contained data from 27 participants collectively, it did contain a robust set of time synchronized IMU recordings from 12 body locations and more than 30 different activities.

As we have acknowledged earlier, the publicly available data we evaluated in this study emanated from two previously conducted studies using IMUs not developed, sold, or marketed by Catapult. Therefore, we do not have a clear picture of PlayerLoad™'s reliability across different brands of IMUs or accelerometers. Unfortunately, the proprietary nature of some aspects of the PlayerLoad™ metric (e.g., why is the Euclidean norm of change in acceleration reduced by one order of magnitude?) detracts from its potential usefulness. ActiGraph activity counts share some similarities in this sense with PlayerLoad™ as it too is a proprietary metric whose formulation was not well understood until more recently (Brønd et al., 2017; Peach et al., 2014). A greater understanding of the exact methods and calculation of Catapult's proprietary PlayerLoad™ would allow researchers in human movement assessment to evaluate the

usefulness of the metric more aptly and potentially offer different routes to improve the usability and generalizability of the metric.

# Chapter 6. Conclusion

In summary, this study utilized two different publicly available wearable monitor data sets (REALDISP and MHEALTH) to quantify, evaluate, and compare associations between Catapult's PlayerLoad™ metric and several other common acceleration metrics typically used in physical activity research (e.g., VMLFE, VMNF, BFEN, ENMO). Observed data supported our primary hypothesis that PlayerLoad™ would be strongly associated with these measures. Of note, associations for PlayerLoad™ with BFEN and ENMO were quite strong ($r$ = 0.742 to 0.983) and of a significantly greater magnitude than PlayerLoad™ associations with VMLFE and VMNF ($r$ = 0.539 - 0.840) in all instances evaluated herein.

Using back- and wrist-positioned IMU data from the REALDISP and MHEALTH studies, respectively, we developed models for predicting PlayerLoad™ from the common BFEN and ENMO metrics used extensively in physical activity research. Moreover, as the associations between these metrics were quite strong, we algebraically rearranged the prediction equations to predict BFEN or ENMO from PlayerLoad™. Model validation using Harrell's optimism bootstrap (Harrell et al., 1996) for predictive indices provided greater evidence of the robustness of our fitted models. Unbiased pseudo $R^2$ values were high for all models and never dropped below 0.879. However, these models were calibrated on epoch level data and as such are only generalizable for epoch- or summary-level predictions. When working with raw triaxial acceleration data it would still be preferable to compute desired metrics using the appropriate formulation as opposed to relying on a prediction equation.

More research is needed to better understand PlayerLoad™ and its potential value for quantifying time-based dosages of human movement. A logical next step would be to compare energy expenditure-related associations between PlayerLoad™, VMLFE, VMNF, BFEN, and

ENMO. The metric(s) demonstrating the strongest associations with energy expenditure would likely prove most useful for tracking dosage of activity in both sport and public health-related contexts.

# BIBLIOGRAPHY

Aguiar, M. V., Botelho, G. M., Gonçalves, B. S., & Sampaio, J. E. (2013). Physiological responses and activity profiles of football small-sided games. *Journal of Strength & Conditioning Research, 27*(5), 1287-1294. doi:10.1519/JSC.0b013e318267a35c

Ainsworth, B., Cahalin, L., Buman, M., & Ross, R. (2015). The current state of physical activity assessment tools. *Progress in Cardiovascular Diseases, 57*(4), 387-395. doi:10.1016/j.pcad.2014.10.005

American College of Sports Medicine. (2018). *ACSM's guidelines for exercise testing and prescription* (Tenth ed.). Philadelphia, PA: Wolters Kluwer Health.

Åstrand, P., Rodahl, K., Dahl, H. A., & Strømme, S. B. (2003). *Textbook of work physiology* (Fourth ed.). Champaign, IL: Human Kinetics.

Bakdash, J. Z., & Marusich, L. R. (2017). Repeated measures correlation. *Frontiers in Psychology, 8*(456). doi:10.3389/fpsyg.2017.00456

Banos, O., Damas, M., Pomares, H., Rojas, I., Tóth, M., & Amft, O. (2012). *A benchmark dataset to evaluate sensor displacement in activity recognition.* Paper presented at the 2012 ACM Conference on Ubiquitous Computing, Pittsburgh, PA.

Banos, O., Garcia, R., Holgado-Terriza, J. A., Damas, M., Pomares, H., Rojas, I., . . . Villalonga, C. (2014). *mHealthDroid: A novel framework for agile development of mobile health applications.* Paper presented at the 6th International Work-Conference, IWAAL: International Workshop on Ambient Assisted Living, Belfast, Northern Ireland.

Banos, O., Toth, M. A., Damas, M., Pomares, H., & Rojas, I. (2014). Dealing with the effects of sensor displacement in wearable activity recognition. *Sensors (Basel), 14*(6), 9995-10023. doi:10.3390/s140609995

Banos, O., Villalonga, C., Garcia, R., Saez, A., Damas, M., Holgado-Terriza, J. A., . . . Rojas, I. (2015). Design, implementation and validation of a novel open framework for agile development of mobile health applications. *BioMedical Engineering Online, 14*(Suppl 2), S6. doi:10.1186/1475-925x-14-s2-s6

Barrett, S., Midgley, A., & Lovell, R. (2014). PlayerLoad™: Reliability, convergent validity, and influence of unit position during treadmill running. *International Journal of Sports Physiology and Performance, 9*(6), 945-952. doi:10.1123/ijspp.2013-0418

Barrett, S., Midgley, A. W., Towlson, C., Garrett, A., Portas, M., & Lovell, R. (2016). Within-match PlayerLoad patterns during a simulated soccer match: Potential implications for unit positioning and fatigue management. *International Journal of Sports Physiology and Performance, 11*(1), 135-140. doi:10.1123/ijspp.2014-0582

Barron, D. J., Atkins, S., Edmundson, C., & Fewtrell, D. (2014). Accelerometer derived load according to playing position in competitive youth soccer. *International Journal of Performance Analysis in Sport, 14*(3), 734-743. doi:10.1080/24748668.2014.11868754

Bassett, D. R., Jr., & Strath, S. J. (2002). Use of pedometers to assess physical activity. In G. Welk (Ed.), *Physical activity assessments for health-related research* (pp. 163-178). Champaign, IL: Human Kinetics.

Beato, M., Devereux, G., & Stiff, A. (2018). Validity and reliability of global positioning system units (STATSports viper) for measuring distance and peak speed in sports. *Journal of*

*Strength and Conditioning Research, 32*(10), 2831-2837. doi:10.1519/JSC.0000000000002778

Benedetto, S., Caldato, C., Bazzan, E., Greenwood, D. C., Pensabene, V., & Actis, P. (2018). Assessment of the Fitbit Charge 2 for monitoring heart rate. *PLoS One, 13*(2), e0192691. doi:10.1371/journal.pone.0192691

Bini, R. R., Diefenthaeler, F., & Carpes, F. P. (2014). Determining force and power in cycling: A review of methods and instruments for pedal force and crank torque measurements. *International SportMed Journal, 15*(1), 96-112. doi:10520/EJC151085

Bot, S. D. M., & Hollander, A. P. (2000). The relationship between heart rate and oxygen uptake during non-steady state exercise. *Ergonomics, 43*(10), 1578-1592. doi:10.1080/001401300750004005

Boyd, L. J., Ball, K., & Aughey, R. J. (2011). The reliability of MinimaxX accelerometers for measuring physical activity in Australian football. *International Journal of Sports Physiology and Performance, 6*(3), 311-321. doi:10.1123/ijspp.6.3.311

Brage, S., Brage, N., Franks, P. W., Ekelund, U., & Wareham, N. J. (2005). Reliability and validity of the combined heart rate and movement sensor Actiheart. *European Journal of Clinical Nutrition, 59*(4), 561-570. doi:10.1038/sj.ejcn.1602118

Bredt, S., Chagas, M. H., Peixoto, G. H., Menzel, H. J., & de Andrade, A. G. P. (2020). Understanding Player Load: Meanings and limitations. *Journal of Human Kinetics, 71,* 5-9. doi:10.2478/hukin-2019-0072

Brønd, J. C., Andersen, L. B., & Arvidsson, D. (2017). Generating ActiGraph counts from raw acceleration recorded by an alternative monitor. *Medicine & Science in Sports & Exercise, 49*(11), 2351-2360. doi:10.1249/mss.0000000000001344

Buchheit, M., Gray, A., & Morin, J. B. (2015). Assessing stride variables and vertical stiffness with GPS-embedded accelerometers: Preliminary insights for the monitoring of neuromuscular fatigue on the field. *Journal of Sports Science and Medicine, 14*(4), 698-701.

Bullock, G. S., Schmitt, A. C., Chasse, P., Little, B. A., Diehl, L. H., & Butler, R. J. (2019). Differences in PlayerLoad and pitch type in collegiate baseball players. *Sports Biomechanics,* Advance Online Publication. doi:10.1080/14763141.2019.1618899

Cain, K. L., Conway, T. L., Adams, M. A., Husak, L. E., & Sallis, J. F. (2013). Comparison of older and newer generations of ActiGraph accelerometers with the normal filter and the low frequency extension. *International Journal of Behavioral Nutrition and Physical Activity, 10*, 51. doi:10.1186/1479-5868-10-51

Calabro, M. A., Welk, G. J., & Eisenmann, J. C. (2009). Validation of the SenseWear Pro Armband algorithms in children. *Medicine & Science in Sports & Exercise, 41*(9), 1714-1720. doi:10.1249/MSS.0b013e3181a071cf

Camomilla, V., Bergamini, E., Fantozzi, S., & Vannozzi, G. (2018). Trends supporting the in-field use of wearable inertial sensors for sport performance evaluation: A systematic review. *Sensors, 18*(3), 873. doi:10.3390/s18030873

Casamichana, D., Castellano, J., & Dellal, A. (2013). Influence of different training regimes on physical and physiological demands during small-sided soccer games: continuous vs. intermittent format. *Journal of Strength and Conditioning Research, 27*(3), 690-697. doi:10.1519/JSC.0b013e31825d99dc

Catapult. (2019). Catapult reaches milestone of 2,500 clients. Retrieved from https://www.catapultsports.com/blog/catapult-reaches-milestone-of-2500-clients

Cavagna, G., Saibene, F., & Margaria, R. (1961). A three-dimensional accelerometer for analyzing body movements. *Journal of Applied Physiology, 16*(1), 191. doi:10.1152/jappl.1961.16.1.191

Chen, K. Y., & Bassett, D. R. (2005). The technology of accelerometry-based activity monitors: Current and future. *Medicine & Science in Sports & Exercise, 37*(11), S490-S500. doi:10.1249/01.mss.0000185571.49104.82

Cleveland, W. S. (1993). *Visualizing data*. United States of America: AT&T Bell Laboratories.

Cohen, J. (1988). *Statistical power analysis for the behavioral sciences*. New Jersey: Lawrence Erlbaum Associates.

Colby, M. J., Dawson, B., Heasman, J., Rogalski, B., & Gabbett, T. J. (2014). Accelerometer and GPS-derived running loads and injury risk in elite australian footballers. *Journal of Strength & Conditioning Research, 28*(8), 2244-2252. doi:10.1519/jsc.0000000000000362

Contini, R., Gage, H., & Drillis, R. (1965). *Human gait characteristics.* Paper presented at the Biomechanics and Related Bio-Engineering Topics Symposium, Glasgow, Scotland.

Coutts, A. J., & Duffield, R. (2010). Validity and reliability of GPS devices for measuring movement demands of team sports. *Journal of Science and Medicine in Sport, 13*(1), 133-135. doi:10.1016/j.jsams.2008.09.015

Crouter, S. E., Churilla, J. R., & Bassett, D. R., Jr. (2008). Accuracy of the Actiheart for the assessment of energy expenditure in adults. *European Journal of Clinical Nutrition, 62*(6), 704-711. doi:10.1038/sj.ejcn.1602766

Delaney, J. A., Wileman, T. M., Perry, N. J., Thornton, H. R., Moresi, M. P., & Duthie, G. M. (2019). The validity of a global navigation satellite system of quantifying small-area

team-sport movements. *Journal of Strength and Conditioning Research, 33*(6), 1463-1466. doi:10.1519/JSC.0000000000003157

Drenowatz, C., & Eisenmann, J. C. (2011). Validation of the SenseWear Armband at high intensity exercise. *European Journal of Applied Physiology, 111*(5), 883-887. doi:10.1007/s00421-010-1695-0

Duncan, M. J., Badland, H. M., & Mummery, W. K. (2009). Applying GPS to enhance understanding of transport-related physical activity. *Journal of Science and Medicine in Sport, 12*(5), 549-556. doi:10.1016/j.jsams.2008.10.010

European Global Navigation Satellite Systems Agency. (2020). What is GNSS? Retrieved from https://www.gsa.europa.eu/european-gnss/what-gnss

Freedson, P. S., Melanson, E., & Sirard, J. (1998). Calibration of the Computer Science and Applications, Inc. accelerometer. *Medicine & Science in Sports & Exercise, 30*(5), 777-781. doi:10.1097/00005768-199805000-00021

George, T. (1993, June 27). Strength and conditioning coaches: The force is with them. *The New York Times*. Retrieved from https://www.nytimes.com/1993/06/27/sports/pro-football-strength-and-conditioning-coaches-the-force-is-with-them.html

Govus, A. D., Coutts, A., Duffield, R., Murray, A., & Fullagar, H. (2018). Relationship between pretraining subjective wellness measures, player load, and rating-of-perceived-exertion training load in American college football. *International Journal of Sports Physiology and Performance, 13*(1), 95-101. doi:10.1123/ijspp.2016-0714

Harrell, F. E., Lee, K. L., & Mark, D. B. (1996). Tutorial in biostatistics: Multivariable prognostic models. *Statistics in Medicine, 15*, 361-387. doi:10.1002/(SICI)1097-0258(19960229)15:4<361::AID-SIM168>3.0.CO;2-4

Hibbing, P. R., Lamunion, S. R., Kaplan, A. S., & Crouter, S. E. (2018). Estimating energy expenditure with ActiGraph GT9X inertial measurement unit. *Medicine & Science in Sports & Exercise, 50*(5), 1093-1102. doi:10.1249/mss.0000000000001532

Hildebrand, M., VT, V. A. N. H., Hansen, B. H., & Ekelund, U. (2014). Age group comparability of raw accelerometer output from wrist- and hip-worn monitors. *Medicine & Science in Sports & Exercise, 46*(9), 1816-1824. doi:10.1249/mss.0000000000000289

Hulin, B. T., Gabbett, T. J., Johnston, R. D., & Jenkins, D. G. (2017). Wearable microtechnology can accurately identify collision events during professional rugby league match-play. *Journal of Science and Medicine in Sport, 20*(7), 638-642. doi:10.1016/j.jsams.2016.11.006

Humphries, B. J., Newton, R. U., & Wilson, G. J. (1995). The effect of a braking device in reducing the ground impact forces inherent in plyometric training. *International Journal of Sports Medicine, 16*(2), 129-133. doi:10.1055/s-2007-972979

Jahrsdoerfer, M., Giuliano, K., & Stephens, D. (2005). Clinical usefulness of the EASI 12-lead continuous electrocardiographic monitoring system. *Critical Care Nurse, 25*(5), 28-37. doi:10.4037/ccn2005.25.5.28

Jennings, D., Cormack, S., Coutts, A. J., Boyd, L., & Aughey, R. J. (2010). The validity and reliability of GPS units for measuring distance in team sport specific running patterns. *International Journal of Sports Physiology and Performance, 5*(3), 328. doi:10.1123/ijspp.5.3.328

Johannsen, D. L., Calabro, M. A., Stewart, J., Franke, W., Rood, J. C., & Welk, G. J. (2010). Accuracy of armband monitors for measuring daily energy expenditure in healthy adults.

*Medicine & Science in Sports & Exercise, 42*(11), 2134-2140. doi:10.1249/MSS.0b013e3181e0b3ff

John, D., & Freedson, P. (2012). ActiGraph and Actical physical activity monitors: A peek under the hood. *Medicine & Science in Sports & Exercise, 44*(Suppl 1), S86-S89. doi:10.1249/MSS.0b013e3182399f5e

John, D., Miller, R., Kozey-Keadle, S., Caldwell, G., & Freedson, P. (2012). Biomechanical examination of the 'plateau phenomenon' in ActiGraph vertical activity counts. *Physiological Measurement, 33*(2), 219-230. doi:10.1088/0967-3334/33/2/219

Julien, C. (2019). What is PlayerLoad? Retrieved from https://support.catapultsports.com/hc/en-us/articles/360000510795-What-is-PlayerLoad-

Kabai, S. (2007). Gyroscope. Retrieved from http://demonstrations.wolfram.com/Gyroscope/

Keytel, L. R., Goedecke, J. H., Noakes, T. D., Hiiloskorpi, H., Laukkanen, R., van der Merwe, L., & Lambert, E. V. (2005). Prediction of energy expenditure from heart rate monitoring during submaximal exercise. *Journal of Sports Sciences, 23*(3), 289-297. doi:10.1080/02640410470001730089

Kripke, D. F., Mullaney, D. J., Messin, S., & Wyborney, V. G. (1978). Wrist actigraphic measures of sleep and rhythms. *Electroencephalography and Clinical Neurophysiology, 44*(5), 674-676. doi:10.1016/0013-4694(78)90133-5

Kuusniemi, H., Lachapelle, G., & Takala, J. H. (2004). Position and velocity reliability testing in degraded GPS signal environments. *GPS Solutions, 8*, 226-237. doi:10.1007/s10291-004-0113-7

Kyprianou, E., Lolli, L., Haddad, H. A., Salvo, V. D., Varley, M. C., Villanueva, A. M., . . . Weston, M. (2019). A novel approach to assessing validity in sports performance

research: Integrating expert practitioner opinion into the statistical analysis. *Science and Medicine in Football, 3*(4), 333-338. doi:10.1080/24733938.2019.1617433

Leger, L., & Thivierge, M. (1988). Heart rate monitors: Validity, stability, and functionality. *The Physician and Sportsmedicine, 16*(5), 143-151. doi:10.1080/00913847.1988.11709511

Leinonen, A., Ahola, R., Kulmala, J., Hakonen, H., Vähä-Ypyä, H., Herzig, K.-H., . . . Jämsä, T. (2017). Measuring physical activity in free-living conditions—Comparison of three accelerometry-based methods. *Frontiers in Physiology, 7*(681). doi:10.3389/fphys.2016.00681

Li, R. T., Salata, M. J., Rambhia, S., Sheehan, J., & Voos, J. E. (2020). Does overexertion correlate with increased injury? The relationship between player workload and soft tissue injury in professional American football players using wearable technology. *Sports Health 12*(1), 66-73. doi:10.1177/1941738119868477

Luinge, H. J., & Veltink, P. H. (2005). Measuring orientation of human body segments using miniature gyroscopes and accelerometers. *Medical & Biological Engineering & Computing, 43*(2), 273-282. doi:10.1007/bf02345966

Luteberget, L. S., Holme, B. R., & Spencer, M. (2018). Reliability of wearable inertial measurement units to measure physical activity in team handball. *International Journal of Sports Physiology and Performance, 13*(4), 467-473. doi:10.1123/ijspp.2017-0036

McNamara, D. J., Gabbett, T. J., Chapman, P., Naughton, G., & Farhart, P. (2015). Variability of PlayerLoad, bowling velocity, and performance execution in fast bowlers across repeated bowling spells. *International Journal of Sports Physiology and Performance, 10*(8), 1009-1014. doi:10.1123/ijspp.2014-0497

Meng, X. L., Rosenthal, R., & Rubin, D. B. (1992). Comparing correlated correlation coefficients. *Psychological Bulletin, 111*(1), 172-175. doi:10.1037/0033-2909.111.1.172

Migueles, J. H., Delisle Nyström, C., Henriksson, P., Cadenas-Sanchez, C., Ortega, F. B., & Löf, M. (2019). Accelerometer data processing and energy expenditure estimation in preschoolers. *Medicine & Science in Sports & Exercise, 51*(3), 590-598. doi:10.1249/mss.0000000000001797

Montgomery, P. G., Pyne, D. B., & Minahan, C. L. (2010). The physical and physiological demands of basketball training and competition. *International Journal of Sports Physiology and Performance, 5*(1), 75-86. doi:10.1123/ijspp.5.1.75

Montoye, H. J., Washburn, R., Servais, S., Ertl, A., Webster, J. G., & Nagle, F. J. (1983). Estimation of energy expenditure by a portable accelerometer. *Medicine & Science in Sports & Exercise, 15*(5), 403-407.

Mullaney, D. J., Kripke, D. F., & Messin, S. (1980). Wrist-actigraphic estimation of sleep time. *Sleep, 3*(1), 83-92. doi:10.1093/sleep/3.1.83

Murphy, A. J., Wilson, G. J., Pryor, J. F., & Newton, R. U. (1995). Isometric assessment of muscular function: The effect of joint angle. *Journal of Applied Biomechanics, 11*(2), 205-215. doi:10.1123/jab.11.2.205

Murray, A., Buttfield, A., Simpkin, A., Sproule, J., & Tuner, A. P. (2018). Variability of within-step acceleration and daily wellness monitoring in collegiate American football. *Journal of Science and Medicine in Sport, 22*(4), 488-493. doi:10.1016/j.jsams.2018.10.013

Nicolella, D. P., Torres-Ronda, L., Saylor, K. J., & Schelling, X. (2018). Validity and reliability of an accelerometer-based player tracking device. *PLoS One, 13*(2), e0191823. doi:10.1371/journal.pone.0191823

NovAtel Inc. (2020). GLONASS. Retrieved from https://www.novatel.com/an-introduction-to-gnss/chapter-3-satellite-systems/glonass/

Passfield, L., Hopker, J. G., Jobson, S., Friel, D., & Zabala, M. (2017). Knowledge is power: Issues of measuring training and performance in cycling. *Journal of Sports Sciences, 35*(14), 1426-1434. doi:10.1080/02640414.2016.1215504

Peach, D., Van Hoomissen, J., & Callender, H. L. (2014). Exploring the ActiLife(®) filtration algorithm: Converting raw acceleration data to counts. *Physiological Measurement, 35*(12), 2359-2367. doi:10.1088/0967-3334/35/12/2359

Polar. (2017). 40 years of incredible firsts. Retrieved from https://www.polar.com/blog/40-years-of-incredible-firsts-polar-history/

Rahman, M. Z. (2012). Beyond trilateration: GPS positioning geometry and analytical accuracy. In J. Shuanggen (Ed.), *Global navigations satellite systems: Signal, theory, and applications*. Rijeka, Croatia: InTech.

Rampinini, E., Alberti, G., Fiorenza, M., Riggio, M., Sassi, R., Borges, T. O., & Coutts, A. J. (2015). Accuracy of GPS devices for measuring high-intensity running in field-based team sports. *International Journal of Sports Medicine, 36*(1), 49-53. doi:10.1055/s-0034-1385866

Randers, M. B., Nielsen, J. J., Bangsbo, J., & Krustrup, P. (2014). Physiological response and activity profile in recreational small-sided football: No effect of the number of players. *Scandinavian Journal of Medicine and Science in Sports, 24*(Suppl 1), 130-137. doi:10.1111/sms.12232

Roe, G., Darrall-Jones, J., Black, C., Shaw, W., Till, K., & Jones, B. (2017). Validity of 10-Hz GPS and timing gates for assessing maximum velocity in professional rugby union

players. *International Journal of Sports Physiology and Performance, 12*(6), 836-839. doi:10.1123/ijspp.2016-0256

Roell, M., Roecker, K., Gehring, D., Mahler, H., & Gollhofer, A. (2018). Player monitoring in indoor team sports: Concurrent validity of inertial measurment units to quanitfy average and peak acceleration values. *Frontiers in Physiology 9*, 141. doi:10.3389/fphys.2018.00141

Rowlands, A. V., Mirkes, E. M., Yates, T., Clemes, S., Davies, M., Khunti, K., & Edwardson, C. L. (2018). Accelerometer-assessed physical activity in epidemiology: Are monitors equivalent? *Medicine & Science in Sports & Exercise, 50*(2), 257-265. doi:10.1249/mss.0000000000001435

Sabatini, A. M. (2005). Quaternion-based strap-down integration method for applications of inertial sensing to gait analysis. *Medical & Biological Engineering & Computing, 43*(1), 94-101. doi:10.1007/bf02345128

Sabatini, A. M. (2011). Estimating three-dimensional orientation of human body parts by inertial/magnetic sensing. *Sensors, 11*(2), 1489-1525. doi:10.3390/s110201489

Sampson, J. A., Murray, A., Williams, S., Halseth, T., Hanisch, J., & Golden, G. (2018). Injury risk-workload associations in NCAA American college football. *Journal of Science and Medicine in Sport, 21*(12), 1215-1220. doi:10.1016/j.jsams.2018.05.019

Sasaki, J. E., da Silva, K. S., Gonçalves Galdino da Costa, B., & John, D. (2016). Measurement of physical activity using accelerometers. In J. K. Luiselli & A. J. Fischer (Eds.), *Computer-Assisted and Web-Based Innovations in Psychology, Special Education, and Health* (pp. 33-60). San Diego: Academic Press.

Schaefer, C. A., Nigg, C. R., Hill, J. O., Brink, L. A., & Browning, R. C. (2014). Establishing and evaluating wrist cutpoints for the GENEActiv accelerometer in youth. *Medicine & Science in Sports & Exercise, 46*(4), 826-833. doi:10.1249/mss.0000000000000150

Schelling, X., & Torres, L. (2016). Accelerometer load profiles for basketball-specific drills in elite players. *Journal of Sports Science and Medicine, 15*(4), 585-591.

Schutz, Y., & Chambaz, A. (1997). Could a satellite-based navigation system (GPS) be used to assess the physical activity of individuals on earth? *European Journal of Clinical Nutrition, 51*(5), 338-339. doi:10.1038/sj.ejcn.1600403

Servais, S. B., Webster, J. G., & Montoye, H. J. (1984). Estimating human energy expenditure using an accelerometer device. *Journal of Clinical Engineering, 9*(2), 159-170.

Shurley, J., & Todd, J. S. (2012). "The Strength of Nebraska": Boyd Epley, Husker power, and formation of the strength and coaching profession. *The Journal of Strength and Conditioning Research, 26*(12), 3177-3188. doi:10.1519/JSC.0b013e31823c4690

Silver, N. C., Hittner, J. B., & May, K. (2004). Testing dependent correlations with nonoverlapping variables: A monte carlo simulation. *The Journal of Experimental Education, 73*(1), 53-69. doi:10.3200/JEXE.71.1.53-70

SRM GMBH. (2015). Our story of success: From the first PowerMeter to the gold standard of power measurement. Retrieved from http://www.srm.de/company/history/

Starlino Electronics. (2009). A guide to using IMU (accelerometer and gyroscope devices) in embedded applications. Retrieved from http://www.starlino.com/imu_guide.html

Staudenmayer, J., Pober, D., Crouter, S., Bassett, D., & Freedson, P. (2009). An artificial neural network to estimate physical activity energy expenditure and identify physical activity

type from an accelerometer. *Journal of Applied Physiology, 107*(4), 1300-1307. doi:10.1152/japplphysiol.00465.2009

Staunton, C., Wundersitz, D., Gordon, B., & Kingsley, M. (2017). Construct validity of accelerometry-derived force to quantify basketball movement patterns. *International Journal of Sports Medicine, 38*(14), 1090-1096. doi:10.1055/s-0043-119224

Stone, M. R., Rowlands, A. V., & Eston, R. G. (2009). Relationships between accelerometer-assessed physical activity and health in children: Impact of the activity-intensity classification method. *Journal of Sports Science and Medicine, 8*(1), 136-143.

Straker, L., & Campbell, A. (2012). Translation equations to compare ActiGraph GT3X and Actical accelerometers activity counts. *BMC Medical Research Methodology, 12*, 54. doi:10.1186/1471-2288-12-54

Swartz, A. M., Strath, S. J., Bassett, D. R., Jr., O'Brien, W. L., King, G. A., & Ainsworth, B. E. (2000). Estimation of energy expenditure using CSA accelerometers at hip and wrist sites. *Medicine & Science in Sports & Exercise, 32*(Suppl 9), S450-S456. doi:10.1097/00005768-200009001-00003

Tamura, T., Maeda, Y., Sekine, M., & Yoshida, M. (2014). Wearable photoplethysmographic sensors-past and present. *Electronics, 3*(2), 282-302. doi:10.3390/electronics3020282

Taylor, E. F., & Wheeler, J. A. (1992). *Spacetime physics: Introduction to special relativity* (Second ed.). New York: W.H. Freeman and Company.

Terbizan, D. J., Dolezal, B. A., & Albano, C. (2002). Validity of seven commercially available heart rate monitors. *Measurement in Physical Education and Exercise Science, 6*(4), 243-247. doi:10.1207/S15327841MPEE0604_3

Thornton, H. R., Nelson, A. R., Delaney, J. A., Serpiello, F. R., & Duthie, G. M. (2019). Interunit reliability and effect of data-processing methods of global positioning systems. *International Journal of Sports Physiology and Performance, 14*(4), 432-438. doi:10.1123/ijspp.2018-0273

Troped, P. J., Wilson, J. S., Matthews, C. E., Cromley, E. K., & Melly, S. J. (2010). The built environment and location-based physical activity. *American Journal of Preventive Medicine, 38*(4), 429-438. doi:10.1016/j.amepre.2009.12.032

Tukey, J. W. (1977). *Exploratory data analysis*. Reading, MA: Addison-Wesley.

Unick, J. L., Bond, D. S., Jakicic, J. M., Vithiananthan, S., Ryder, B. A., Roye, G. D., . . . Wing, R. R. (2012). Comparison of two objective monitors for assessing physical activity and sedentary behaviors in bariatric surgery patients. *Obesity Surgery, 22*(3), 347-352. doi:10.1007/s11695-011-0491-1

United States Department of Defense. (2008). *Global Positioning System Standard Positioning Service Performance Standard*. United States Department of Defense, Retrieved from https://www.gps.gov/technical/ps/2008-SPS-performance-standard.pdf

United States Space Force. (2020). Space Force decommissions 26-year-old GPS satellite to make way for GPSIII constellation. Retrieved from https://www.spaceforce.mil/News/Article/2071281/space-force-decommissions-26-year-old-gps-satellite-to-make-way-for-gpsiii-cons

van Hees, V. T., Fang, Z., Langford, J., Assah, F., Mohammad, A., da Silva, I. C., . . . Brage, S. (2014). Autocalibration of accelerometer data for free-living physical activity assessment using local gravity and temperature: an evaluation on four continents. *Journal of Applied Physiology, 117*(7), 738-744. doi:10.1152/japplphysiol.00421.2014

van Hees, V. T., Gorzelniak, L., Dean León, E. C., Eder, M., Pias, M., Taherian, S., . . . Brage, S. (2013). Separating movement and gravity components in an acceleration signal and implications for the assessment of human daily physical activity. *PLoS One, 8*(4), e61691. doi:10.1371/journal.pone.0061691

Van Iterson, E. H., Fitzgerald, J. S., Dietz, C. C., Snyder, E. M., & Peterson, B. J. (2017). Reliability of triaxial acceleromtery for measuring load in men's collegiate ice hockey. *Journal of Strength and Conditioning Research, 31*(5), 1305-1312. doi:10.1519/JSC.0000000000001611.

van Loo, C. M. T., Okely, A. D., Batterham, M. J., Hinkley, T., Ekelund, U., Brage, S., . . . Cliff, D. P. (2018). Wrist acceleration cut points for moderate-to-vigorous physical activity in youth. *Medicine & Science in Sports & Exercise, 50*(3), 609-616. doi:10.1249/mss.0000000000001449

Wallen, M. P., Gomersall, S. R., Keating, S. E., Wisloff, U., & Coombes, J. S. (2016). Accuracy of heart rate watches: Implications for weight management. *PLoS One, 11*(5), e0154420. doi:10.1371/journal.pone.0154420

Watson, K. B., Carlson, S. A., Carroll, D. D., & Fulton, J. E. (2014). Comparison of accelerometer cut points to estimate physical activity in US adults. *Journal of Sports Sciences, 32*(7), 660-669. doi:10.1080/02640414.2013.847278

Welch, W. A., Bassett, D. R., Thompson, D. L., Freedson, P. S., Staudenmayer, J. W., John, D., . . . Fitzhugh, E. C. (2013). Classification accuracy of the wrist-worn gravity estimator of normal everyday activity accelerometer. *Medicine & Science in Sports & Exercise, 45*(10), 2012-2019. doi:10.1249/MSS.0b013e3182965249

Wellman, A. D., Coad, S. C., Flynn, P. J., Siam, T. K., & McLellan, C. P. (2019). Perceived wellness associated with practice and competition in national acollegiate athletic association division I football players. *Journal of Strength and Conditioning Research 33*(1), 112-124. doi:10.1519/JSC.0000000000002169

Wik, E. H., Luteberget, L. S., & Spencer, M. (2017). Activity profiles in international women's team handball using PlayerLoad. *International Journal of Sports Physiology and Performance, 12*(7), 934-942. doi:10.1123/ijspp.2015-0732

Witte, T. H., & Wilson, A. M. (2004). Accuracy of non-differential GPS for the determination of speed over ground. *Journal of Biomechanics, 37*(12), 1891-1898. doi:10.1016/j.jbiomech.2004.02.031

Wolff-Hughes, D. L., Troiano, R. P., Boyer, W. R., Fitzhugh, E. C., & McClain, J. J. (2016). Use of population-referenced total activity counts percentiles to assess and classify physical activity of population groups. *Preventive Medicine, 87,* 35-40. doi:10.1016/j.ypmed.2016.02.019

Wong, T. C., Webster, J. G., Montoye, H. J., & Washburn, R. (1981). Portable accelerometer device for measuring human energy expenditure. *IEEE Transactions on Biomedical Engineering, 28*(6), 467-471. doi:10.1109/TBME.1981.324820

Xiao, L., He, B., Koster, A., Caserotti, P., Lange-Maia, B., Glynn, N. W., . . . Crainiceanu, C. M. (2016). Movement prediction using accelerometers in a human population. *Biometrics, 72*(2), 513-524. doi:10.1111/biom.12382

You, Z. (2017). *Space microsystems and micro/nano satellites*. Cambridge: Massachusetts: Elsevier.

Young, C. M., Gastin, P. B., Sanders, N., Mackey, L., & Dwyer, D. B. (2016). Player Load in elite netball: Match, training, and positional comparisons. *International Journal of Sports Physiology and Performance, 11*(8), 1074-1079. doi:10.1123/ijspp.2015-0156

Zhang, Z., Pi, Z., & Liu, B. (2015). TROIKA: A general framework for heart rate monitoring using wrist-type photoplethysmographic signals during intensive physical exercise. *IEEE Transactions on Biomedical Engineering, 62*(2), 522-531. doi:10.1109/TBME.2014.2359372

Zhihua, T. (2008). *The Application of GPS/GIS Navigation and Positioning System in Cross-Country Orienteering.* Paper presented at the 2008 International Conference on Computer Science and Software Engineering.

# APPENDICES

# Appendix A. Institutional Review Board Determination

Oregon State University
Research Office

Human Research Protection Program
& Institutional Review Board
B308 Kerr Administration Bldg, Corvallis OR 97331
(541) 737-8008
IRB@oregonstate.edu
http://research.oregonstate.edu/irb

| | | | |
|---|---|---|---|
| Date of Notification | April 24, 2020 | Study Number | IRB-2020-0645 |
| Notification Type | Oversight Determination | | |
| Principal Investigator | John M Schuna Jr | | |
| Study Team Members | Dailey, Dakota B; | | |
| Study Title | A comparison of three metrics for quantifying human movement using inertial movement units. | | |
| Funding Source | None | Cayuse Number | N/A |

**DETERMINATION:** RESEARCH, BUT NO HUMAN SUBJECTS

It has been determined that your project, as submitted, does meet the definition of research but **does not** involve human subjects under the regulations set forth by the Department of Health and Human Services 45 CFR 46.

Additional review is not required for this study.

Please do not include HRPP contact information on any of your study materials.

**Note that amendments to this project may impact this determination. Please submit a *new* request if there are changes (e.g., funding, data sources, access to individual identifiers, interaction with research subjects, etc.).**

The federal definitions and guidance used to make this determination may be found at the following link: Human Subject

## Appendix B. Prediction Equations

| Data Set | Location | Predict PlayerLoad™, BFEN, or ENMO |
|---|---|---|
| **REALDISP** | **Back** | $PlayerLoad^{0.484} = BFEN \times 0.0011 + 0.3411$ |
| **REALDISP** | **Back** | $PlayerLoad^{0.698} = ENMO \times 0.0029 + 0.3170$ |
| **MHEALTH** | **Wrist** | $PlayerLoad^{0.590} = BFEN \times 0.0010 + 0.2969$ |
| **MHEALTH** | **Wrist** | $PlayerLoad^{1.636} = ENMO \times 0.0065 - 0.1561$ |
| | | |
| **REALDISP** | **Back** | $BFEN = (PlayerLoad^{0.484} - 0.3411) \times (1/0.0011)$ |
| **REALDISP** | **Back** | $ENMO = (PlayerLoad^{0.698} - 0.3170) \times (1/0.0029)$ |
| **MHEALTH** | **Wrist** | $BFEN = (PlayerLoad^{0.590} - 0.2969) \times (1/0.0010)$ |
| **MHEALTH** | **Wrist** | $ENMO = (PlayerLoad^{1.636} + 0.1561) \times (1/0.0065)$ |